POLITECNICO DI MILANO

School of Civil, Environmental and Land Management Engineering

Master of Science in Environmental and Land Planning Engineering

Advancing reservoir operation description in physically based hydrological models

Supervisor:
Prof. Andrea Castelletti

Assistant Supervisors:
Dr. Daniela Anghileri
Prof. Paolo Burlando

Master Graduation Thesis by:

Federico Giudici
Student Id n. 819769

Academic Year 2014-2015

Acknowledgments

First of all I would like to thank Professor Andrea Castelletti who gave me the opportunity to deepen my interest in water resources management, supporting and helping me with his valuable advices.

I would like to express my sincere gratitude to Daniela Anghileri for her patience, motivation, enthusiasm, and knowledge. She provided me her incessant assistance along all these months, guiding me in the right direction and encouraging me during the difficult times. My research would not have been possible without her help.

I would like to thank Professor Paolo Burlando, who hosted me in Zurich at the department of Hydrology and Water Resources Management of ETH, giving me the possibility to work in an exciting and challenging environment, in close contact with brilliant researchers.

I'm also very grateful to Enrico Weber: I really appreciated his important contribute and knowledge in developing some of the most technical issues of this thesis.

Besides the academic support, all my family has been essential to achieve this important goal. In particular I would like to thank my parents, my grandmothers and my uncles for their constant presence and their unconditional trust across these years of university.
Moreover, I would express a loving thank to Beatrice, who was always close to me with patience and sensibility during all this experience.

Table of Contents

List of figures

List of tables

Abstract

The evolution of physically based hydrological models in recent years significantly improved our ability to describe and represent the hydrological processes at the basin scale. However, when the modelled system is strongly affected by a human component, which alters the natural water cycle, the performance of these models decrease: as they generally describe the human behaviour through simple operating rules, which are not able to fully capture the complexity of the operators' decision-making processes.

In this thesis, we analyse a typical Coupled Human Natural System (CHNS), in which the human and the natural components interact and co-evolve in space and time. In particular, we focus on an alpine basin, where the natural hydrological cycle is deeply influenced by the presence of several hydroelectric reservoirs.

Our goal is to integrate, within a distributed and physically based hydrological model, a behavioural model that can accurately describe the decision-making processes of hydroelectric operators. In so doing, we can assess how the level of detail in the description of the human component affects the overall model accuracy.

We also want to assess how simple and complex reservoirs operating rules are able to represent the system evolution in a changing context: in particular, we focus on changes in socio-economic drivers, considering different energy price scenarios.

The hydrological model used is Topkapi-ETH, a spatially distributed and physically based model, which allows to implement anthropogenic structures such as hydroelectric reservoirs and river diversions, providing the hydrological response of the system at any location of the basin. Topkapi-ETH allows simulating the reservoirs dynamic with simple operating rules, based on the definition of a target level, which usually represents the trajectory of reservoir level during a normal hydrological year and it is derived from historical observations.

The behavioural model of hydroelectric operators is implemented using an implicit model based on Stochastic Dynamic Programming (SDP), which can calculate optimized management policies.

Results show how the use of optimized policies for the description of the hydroelectric operator's behaviour allows to obtain better results with respect to the use of simple operating rules based on historical observations. The variability of the flow observed in different sections of the basin is not represented by the model when the reservoirs are simulated with the use of simple operating rules, but it is instead captured with the use of optimized management policies, which define the release decisions based on the variability of the energy price.

The use of optimized policies also allows predicting the behaviour of the system in response to changes in climate and socio-economic drivers, adapting the behaviour of hydroelectric reservoirs to the new boundary conditions. The simple management rules, based on the observation of historical data, suffer instead from a structural delay in anticipating the effects of these changes: the observation of the system under the new

boundary conditions is in fact essential to define the new dynamics of hydroelectric reservoirs.
Potential development of this thesis aims to test simple and complex reservoirs operating rules under different future scenarios (e.g., climate change). Since results show that the effects of the anthropic component on the hydrology are not local but are distributed throughout the basin, it would be interesting integrate advanced reservoirs operating rules also in global scale hydrological models, in order to evaluate the human influences on the continental and global water cycles.

Riassunto

Negli ultimi anni l'evoluzione dei modelli idrologici fisicamente basati ha permesso di migliorare considerevolmente la capacità di descrivere e rappresentare i processi idrologici su scala di bacino. Tuttavia, quando nel sistema è presente una forte componente antropica, che agisce alterando il naturale ciclo idrologico, le prestazioni di tali modelli diminuiscono: essi infatti modellizzano il comportamento umano attraverso semplici regole operative che non sono in grado di rappresentare la complessità dei processi decisionali degli operatori.

In questa tesi analizziamo un tipico Coupled Human Natural System (CHNS), nel quale la componente umana e quella naturale interagiscono reciprocamente e co-evolvono nello spazio e nel tempo. In particolare, ci focalizziamo su un bacino alpino in cui il ciclo idrologico naturale è profondamente influenzato dalla presenza di un gran numero di serbatoi idroelettrici.

Il nostro obiettivo è quello di integrare in un modello idrologico distribuito e fisicamente basato, un modello comportamentale in grado di descrivere accuratamente i processi decisionali degli operatori idroelettrici. Possiamo così valutare come il livello di dettaglio nella descrizione della componente antropica incide sull'accuratezza del modello.

Vogliamo inoltre valutare come regole operative di gestione dei serbatoi semplici e complesse sono in grado di rappresentare i possibili effetti sul sistema in contesti di cambiamento. In particolare ci focalizziamo su cambiamenti nei driver socio-economici, considerando diversi scenari di prezzo dell'energia.

Il modello idrologico utilizzato è Topkapi-ETH, un modello fisicamente basato e spazialmente distribuito, che permette di implementare strutture antropiche, come serbatoi idroelettrici e gronde, fornendo la risposta idrologica del sistema in ogni area del bacino. Topkapi-ETH consente di simulare la dinamica dei serbatoi con semplici regole operative, basate sulla definizione di un "target level", che rappresenta, solitamente, la traiettoria di livello del serbatoio durante una normale anno idrologico ed è ottenuto da osservazioni storiche.

Il modello comportamentale degli operatori idroelettrici è implementato utilizzando un modello implicito basato sull'algoritmo Stochastic Dynamic Programming (SDP), in grado di calcolare politiche di gestione ottimizzate.

I risultati mostrano come l'utilizzo di politiche ottimizzate per la descrizione del comportamento degli operatori idroelettrici permette di ottenere risultati migliori rispetto all'utilizzo di semplici regole operative basate su osservazioni storiche: la variabilità della portata osservata in diverse sezioni del bacino, non rappresentata dal modello quando i serbatoi sono gestiti con l'uso di semplici regole operative, viene invece catturata con l'utilizzo di politiche di gestione ottimizzate, che definiscono le decisioni di rilascio in base alla variabilità dei prezzi dell'energia.

L'utilizzo di politiche ottimizzate permette inoltre di prevedere le risposte del sistema a fronte di cambiamenti nei driver climatici e socio-economici adattando il comportamento dei serbatoi idroelettrici alle nuove condizioni

al contorno. Le politiche di gestione semplici, basate sulla sola osservazione dei dati storici, soffrono invece di un ritardo strutturale nell'anticipare gli effetti di tali cambiamenti: l'osservazione del sistema sotto le nuove condizioni al contorno è infatti essenziale per definire le nuove dinamiche dei serbatoi idroelettrici.

Potenziali sviluppi di questa tesi potrebbero riguardare la valutazione di regole operative di gestione dei serbatoi semplici e complesse sotto diversi scenari futuri (ad esempio, scenari di cambiamento climatico). Poiché i risultati ottenuti dimostrano che gli effetti della componente antropica sulla idrologia del sistema non sono locali ma sono distribuiti su tutto il bacino, sarebbe interessante integrare regole operative avanzate di gestione dei serbatoi anche in modelli idrologici a scala globale, al fine di valutare le influenze umane sul ciclo dell'acqua a livello continentale e globale.

1 Introduction

The development of hydrological models started from the middle of the 19th century with the goal of understanding and predicting hydrologic phenomena at the catchment scale. Until the first half of the 20th century, hydrology was dominated by approaches that treated catchments as lumped systems or black boxes, with an explicit focus on time [Sivapalan, 2010]. Systems approaches, based for example on the unit hydrograph theory [Dooge, 1955], allows to obtain the catchment response only at the event scale, computing the peak flow starting from rainfall intensity measurements. Empirical approaches and early conceptual models recognize, instead, the time dependency of the catchment responses from seasonal to multi-years [Yevjevich, 1972; Crawford and Linsley, 1966]. When digital computers and new measurements technics became available (e.g., spatial data), the focus shifted from time to space with the aim to capture spatial heterogeneity and improve process resolution [Wood et al., 2011]. This lead to the replacement of empirical and conceptual models with distributed physical based models. The next improvement was then the integration of a range of environmental processes into such models, including chemical, erosional and biological processes [Kumar et al., 2009; Therrien et al., 2010].

With the increasing impact of the human activities on the hydrological cycle, the need to study the human behaviour and the physical and natural processes in an integrated way has raised, in order to capture and understand the strong relationship between human and natural systems [Voisin et al., 2013] but also to more realistically predict the future evolution. This new approach consists in the definition of a coupled system in which the human and the natural components interact each other and co-evolve in space and time (Figure 1-1). Examples of theoretical studies that describe the relationships between human and nature in Coupled Human Natural Systems (CHNS) are various [Falkenmark, 1997; Wagener et al., 2010] but we have few practical applications of this idea, due to the intrinsically complexity of the systems and the difficulties in capturing the interaction and the feedbacks between the components. Examples of such applications in water systems, based on agent based modeling, can be found, for example, in Ng et al., [2011], Barthel et al., [2008], Becu et al., [2003], Giuliani and Castelletti, [2013].

While we have many models that accurately describe physical processes and human behaviour independently, CHNS models are less frequent and are usually more focused on the natural system, at the cost of a simplified description of the human component. This mismatch between the level of detail used to describe the natural processes and the level of detail used to describe the human component become more evident when changes in the external disturbances (e.g., climate change, socio-economical changes) affect the system. In such cases, the stationary assumption of most of the natural systems is removed [Milly et al., 2007] and the simplistic models, which are usually used to describe the human behaviour, are insufficient to capture the feedback and the relationships between natural and human

components.
Alpine catchments represent a paradigmatic example of CHNS. During the XXI century, many artificial reservoirs were constructed for hydropower production, completely altering the natural hydrological regimes by moving large volumes of water in space and time to produce energy when it is more convenient. Distributed physical-based models are able to accurately represent physical processes occurring in the hydrological cycle, but usually describe hydropower infrastructure and their operations with simple models and basic operating rules (e.g., rules tracking how the reservoirs has been operated on average in the past). These rules can usually reproduce the seasonal water volume shift due to the reservoirs' operation, but cannot capture the actual and complex decision making processes, e.g., the influence of energy price and demand on reservoir operation or the different reservoir response in dry or wet conditions. The drawback of modelling human behaviour with those simple operating rules becomes evident when CHNS models are used to assess and anticipate the impacts of changes in climate and socio-economics drivers [Anghileri et al. 2011, Giuliani et al., 2016]. In these cases, understanding and accurately modelling hydropower operators' behaviour is essential to correctly represent the relationships and the feedbacks between natural and human components. Coupling complex behavioural modelling techniques, based on decision-making theory, and accurate hydrological models, in a framework describing the interactions between human and naturals components, is one of the major challenge in the recent study of CHNS.

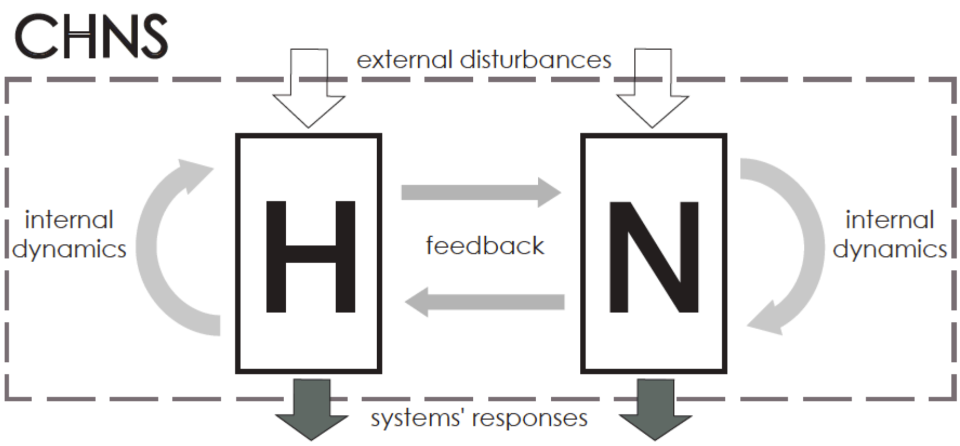

Figure 1-1: The conceptualized diagram of CHNS [Polhill et al., 2016]

1.1 Objectives of the thesis

The main objective of this thesis is to compare the differences that may arise from the inclusion of simple and advanced reservoirs operating rules in CHNS models in order to assess the relationship and the feedbacks that exist between natural and human components.
Distributed physically based hydrological models describe with high level of detail the physical processes occurring in the hydrological cycle, but usually use simple operating rules to take into account the reservoirs

behaviour. These rules are based on the definition of rule-curves representing the behaviour of the reservoir during normal operating conditions and they are estimated from historical observations. These rules are usually able to capture the main dynamics of hydroelectric reservoirs that move large volumes of water in space and time, but don't capture more complex decision-making processes.
We want to test whether increasing the level of detail in the description of the human components within a hydrological model allows obtaining better results in representing the system behaviour.
We therefore implement and integrate, in a fully distributed physically based hydrological model (Topkapi-ETH), advanced reservoirs operating rules, designed by solving an optimization problem, which describe the actual complex decision making process.
We also want evaluate how simple and complex reservoirs operating rules are able to capture the impacts on the system in response to changes in the socio-economic drivers, by considering different energy prices scenarios.
The application of this framework is performed on the water system of Lake Como catchment in the Italian Alps.

1.2 Thesis structure

This thesis is structured in the following chapters:

- Chapter 2 provides a description of the methodology and tools used in this thesis.
- Chapter 3 contains a description of the study area of the Lake Como CHNS.
- Chapter 4 describes the application of the hydrological model Topkapi-ETH to the Lake Como catchment, showing the set up of the hydrological model and the calibration and validation phases.
- Chapter 5 describe the design of the complex reservoir operating rules, e.g., the control problem and the optimization algorithm, showing the results for different electricity prices scenarios.
- Chapter 6 describes the implementation of the simple and complex reservoir operating rules in the hydrological model Topkapi-ETH.
- Chapter 7 shows the results of a comparison between the two reservoir operating rules in terms of effects on the hydrology and hydropower production.

2 Methodology and tools

When dealing with CHNS, describing both natural and human components with the same level of detail is a crucial point to better understand the system and its dynamics.

Distributed physical-based models are able to accurately represent physical processes occurring in the hydrological cycle at the basin scale but usually describe hydroelectric operators behaviour with simple operating rules that can reproduce the seasonal water volume shift due to real reservoir operation, but cannot capture more complex decision making processes in response, e.g., to the fluctuations of energy prices and demands, the temporal unavailability of power plants or varying amount of snow accumulated in the basin.

Since we focus on hydropower production in alpine catchments, the main natural components, that we have to represent, are snow and glaciers' dynamics, and river runoff generation processes; instead, the main anthropic structures are the hydroelectric reservoirs and river diversions.

Figure 2-1 shows how hydroelectric operators' behaviour affects the hydrological cycle through the reservoir release, which is defined on the basis of socio economic variables (energy demand, energy prices), natural variables (inflow forecast, glaciers' dynamics) and operational and normative constraints (min/max production, minimum environmental flow). On the other side, changes in the hydrological cycle involve feedback processes that influence the reservoirs operators' behaviour. For instance, the reservoirs may change the hydraulic and sediment transport characteristics of the river, causing increased potential sedimentation within the storage and depriving the downstream of the sediment material. This excessive sedimentation in the reservoir decreases its water storage capacity, creating important sustainability issues on the long term.

In order to capture the complex interactions between natural and human components, it is important to integrate accurate behavioural models in the hydrological model. There are two main categories of behavioural models (Figure 2-2):

- **Explicit models** (or rule based): they strive on describing and explaining the mechanism of how humans think and make choices, deriving, usually, simple operating rules empirically or from observed data. These models are able to reproduce the past behaviour of the system very well, but, since they are based on historical data, they are affected by a structural delay in capturing system's changes: the observation of the system in response to these changes is, in fact, essential to adapt the model to the new boundary conditions. Therefore, these kinds of models are not usually suitable for prediction (e.g., climate change projections).

- **Implicit models** (or optimisation based): they consider the decision makers as rational agents who maximize (minimize) utility functions. The utility function usually represents measurable criteria that the decision maker uses to rank different decisions/options. These models describe the decision making process as an optimisation problem. They are very flexible in capturing changes in the system, but suffer from the critics about rational agent assumption: some studies report that often humans' behaviour might not be entirely rational [Baron, 1998; Nickerson, 1998].

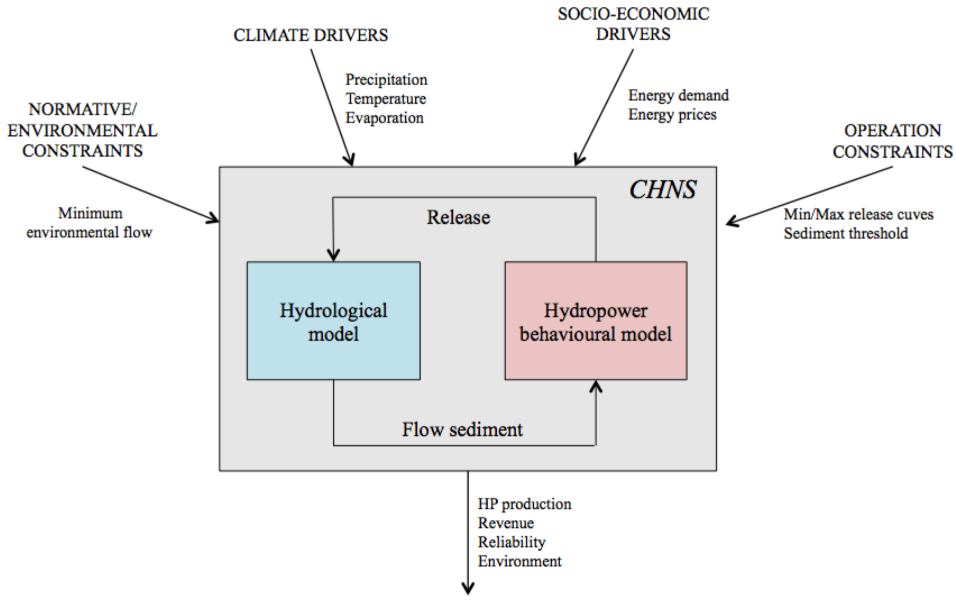

Figure 2-1: Interactions between the hydropower behavioural model and the hydrological model in a CHNS

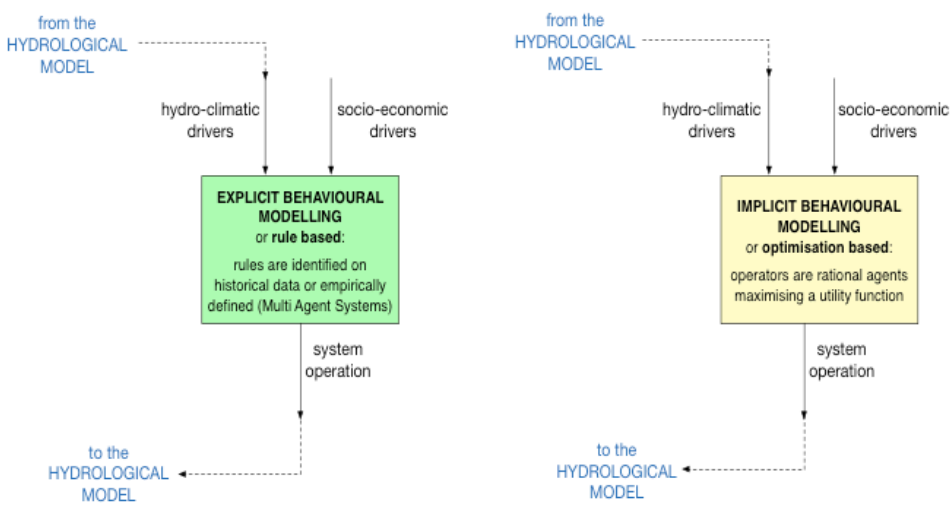

Figure 2-2: Explicit and Implicit behavioural models

The approach proposed in this thesis allows analysing and assessing the effects of simple and complex reservoirs operating rules on the hydrology and on the hydropower system, evaluating their flexibility in capturing changes in natural or socio-economic drivers.

The simple operating rule is obtained from an explicit behavioural model, based on the definition of a target level, which usually represents the trajectory of reservoir level during a normal hydrological year [Soncini-Sessa et al., 2007] and it is derived from historical observation. The operating rule sets the reservoir outflow to zero, when the level is lower then the target trajectory, and to the maximum allow, when the level is bigger then the target trajectory.
This simple operating rule can capture the seasonal water volume shift due to reservoir operation and it's therefore suitable when the focus is on hydrology only.
The main issue of this model is instead related to the definition of the target level, especially when dealing with changing context (e.g., climate change, new renewable energy sources) and when the focus is also on energy: in such case it is better to adopt more complex behavioural models that can reproduce the reservoirs dynamics more accurately.

The complex operating rule used in this thesis is derived from an implicit behavioural model, which solves an optimal control problem via Stochastic Dynamic Programming (SDP). This approach is more suitable in capturing complex reservoirs dynamics.

Implementing models that accurately describe the dynamics and the processes concerning the main natural (e.g., temperature, precipitation, evapotranspiration) and socio-economic (e.g., energy price, energy demand) drivers that influence CHNS is essential to capture the system behaviour in response to possible changes of these drivers.

Changes in *natural drivers* can influence the hydrology of the system in two ways (Figure 2-3):

- *Directly*: changes in meteorological inputs produce changes in the hydrology upstream of the reservoirs.
- *Indirectly:* changes in the hydrology upstream of the reservoir may produce different inflow causing a possible reaction by the operators that could change their policy and therefore affect the hydrology downstream of the reservoir.

On the contrary, changes in *socio-economic drivers* don't affect the hydrology upstream of the reservoirs, but may affect the hydrology downstream of the reservoir through potential changes in the operators' behaviour.

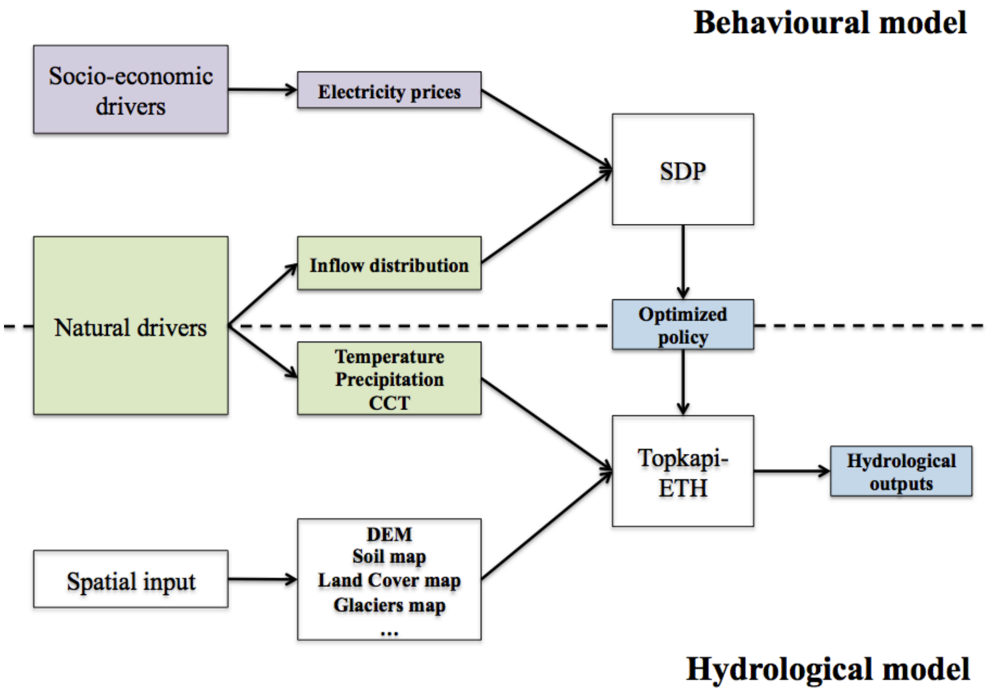

Figure 2-3: Relationship between the hydrological model (Topkapi-ETH) and the behavioural model

In this thesis we focus on changes in the socio-economic drivers, through the definition of different electricity prices scenarios.
The following chapters describe more in details the tools and the scenarios used in this thesis.

2.1 Topkapi-ETH

The hydrological model adopted in this thesis is Topkapi-ETH (Topographic Kinematic Approximation and Integration model), originally developed by Todini and others [Ciarapica and Todini, 2002; Liu and Todini, 2002; Liu and Todini, 2006] and later improved by the department of Hydrology and Water Resources Management (HWRM), in the Institute of Environmental Engineering (IfU) of the Federal Institute of Technology in Zurich.

Topkapi-ETH uses a regular grid where the single grid cell is the smallest computational element. Each grid cell receives water from up to three upstream cells and provides water to a single downstream cell (Figure 2-4). The model is based on a vertical discretization of subsurface in three layers: the deepest one is implemented as a linear reservoirs and mimics the behaviour of slow components such as fractured or porous rock aquifers and the first two layers, implemented as non-linear reservoirs, represents deep and shallow soil. Topographic gradients are used to connect the grid cells in the surface and in subsurface. The potential infiltration is computed with an empirical formula and saturation excess or infiltration processes regulate the runoff. Priestly Taylor equation [Priestley and Taylor, 1972] regulates the evapotraspiration, defined for different land uses through the application a monthly correction factor. Snow and ice-melt are calculated with an empirical temperature index model, which uses only shortwave radiation and air temperature [Pellicciotti et al., 2005; Carenzo et al., 2009]. Unlike other physically-based hydrological models, Topkapi-ETH does not reproduce hydrological processes with high level of detail and complexity [Fatichi et al., 2013] but represents a reasonable compromise between hydrological representation and computational time for large catchments. Moreover the model is able to take into account some anthropogenic infrastructures such as reservoirs, river diversions and water abstractions.

Topkapi-ETH requires the definition of the values of air temperature, cloud cover trasmissivity and precipitation for each grid cell at the temporal and spatial resolution selected for the model simulation. Furthermore, Topkapi-ETH needs a series of spatial inputs for the model setup: a digital elevation map of the catchment, a soil map, a land use map, and a map of the glaciers. The simulated outputs are: water volume in upper subsurface layer, effective saturation in upper subsurface layer, effective saturation in lower subsurface layer, effective saturation in groundwater aquifer, channel flow, flow in upper subsurface layer, flow in lower subsurface.

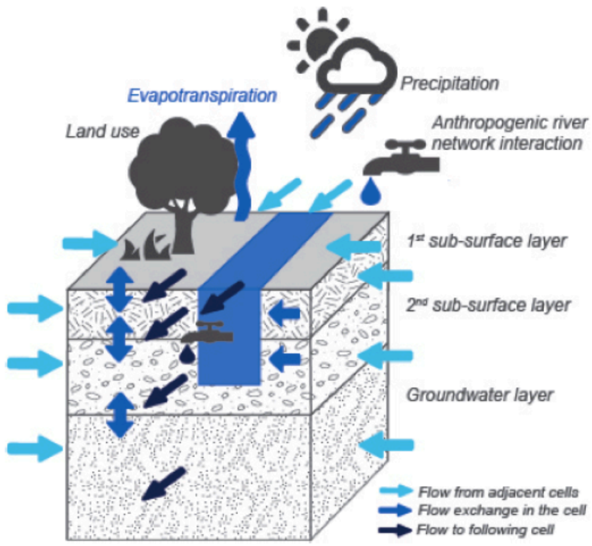

Figure 2-4: Topkapi-ETH structure

2.2 Stochastic Dynamic Programming

We represent the reservoir operation using an implicit behavioural model, based on Stochastic Dynamic Programming (SDP). According to this category of models, the decision maker is represented as a rational agent that wants to maximize an objective function [Soncini-Sessa et al., 2007]. SDP algorithms can solve, under some operating hypothesis, an optimal control problem, generating an optimized policy [Castelletti et al., 2008].

In this thesis a mono-objective, TDC-infinite-horizon SDP algorithm is implemented. The objective function to be maximized is defined as the revenue obtained from the sale of electricity produced by the turbines downstream of the reservoirs.
The application of SDP algorithm for the systems considered in this thesis is provided in chapter 5.

2.3 Electricity prices scenarios

As already mentioned, in this thesis we focus on the behaviour of CNHS in response to changes in the socio-economic drivers, through the definition of different electricity prices scenarios. Since our case study is located in Italy (see chapter 3), in this section we provide an overview of the Italian energy market, with some references to the European situation (chapter 2.3.1) giving, at the end, information about the energy price data used in our analysis (chapter 2.3.2).

2.3.1 The Energy Market

The liberalization of the electricity market has been launched in Italy by the Legislative Decree 16 March 1999, which transposed the information contained in the European Directive No. 92 of 1996 on the creation of an energy market. From 1999 to April 2004, a specific independent authority, called "Autorità per l'Energia Elettrica e il Gas (AEEG)", established a constrained market in which electricity prices, articulated on time slots and months of the year, were defined periodically. In April 2004 the liberalization process of the energy market was completed: the electricity prices are now defined for each hour of each day on the basis of operators' supply and demand. The market is managed by the "Gestore del Mercato Elettrico (GME)". If there is no congestion related to maximum transmission limits of energy in the national grid the so called PUN (Prezzo Unico Nazionale) represents the national energy price, otherwise the market is divided into zones where different prices are defined. The results of this market separation allow energy operators to compete in smaller areas.

The introduction of new Renewable Energy Sources

After the adoption of the 20-20-20 EU Directive (Climate Action and Renewable Energy Package) in 2007, the energy sector is significantly changed with the introduction of new renewable energy sources. This package consists, in fact, in a set of binding legislation to ensure EU meets its climate and energy target for the year 2020. The three key targets are:

- 20% cut in greenhouse gas emissions (from 1990 levels)
- 20% of EU energy from renewables
- 20% improvement in energy efficiency

Figure 2-5 shows the Italian trend in terms of percentage of total energy

consumption produced by renewable sources. It's possible to note a significantly increase of renewable sources starting from 2008. Figure 2-6 shows instead the energy mix of the European country and United States at 2012. The renewable energy mix of Italy accounts for about 30% of the total energy production.
The introduction of new renewable sources might have a great impact on the electricity price. As already explained, the price is determined from the intersection between supply and demand curves. Since the supply curve is organized in Italy according to marginal cost of the technologies, renewable sources, which have almost zero marginal costs of production, displace from the supply curve the traditional systems, less efficient and therefore more expensive, helping to reduce the energy price in the market. This phenomenon is known as merit order effect (Figure 2-7).

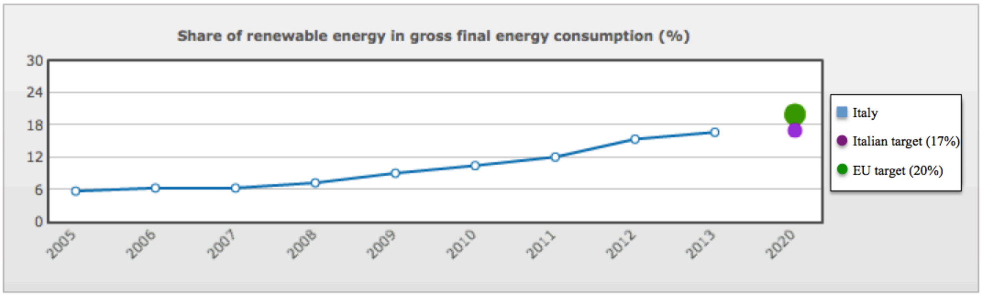

Figure 2-5: Percentage of total energy consumption from renewable sources – Source: European Commission

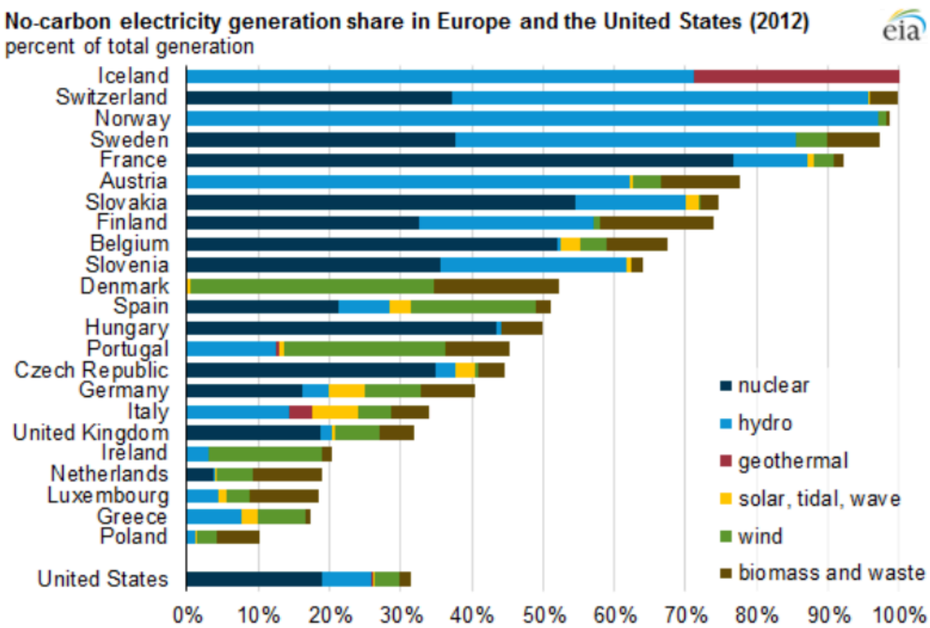

Figure 2-6: New renewable energy sources share in European countries, United States and Italy – Source: U.S. Energy Information Administration, 2012

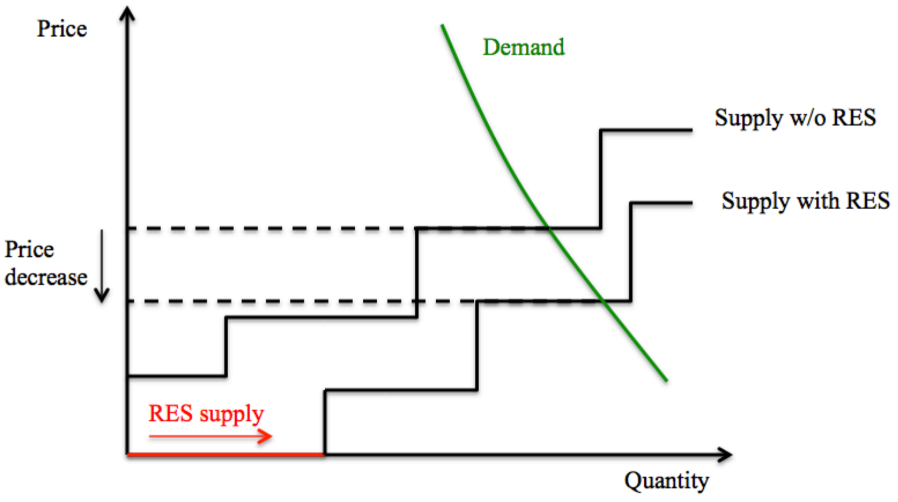

Figure 2-7: Merit order effect diagram

2.3.2 Energy price data

Energy price data used in this thesis are referred to the period 2005-2015. These data are provided by the “Gestore del Mercato Elettrico (GME)”. Figure 2-8 and Figure 2-9 show the PUN daily time series in the pre-renewable period (2005-2008) and in the post-renewable period (2009-2015) respectively.

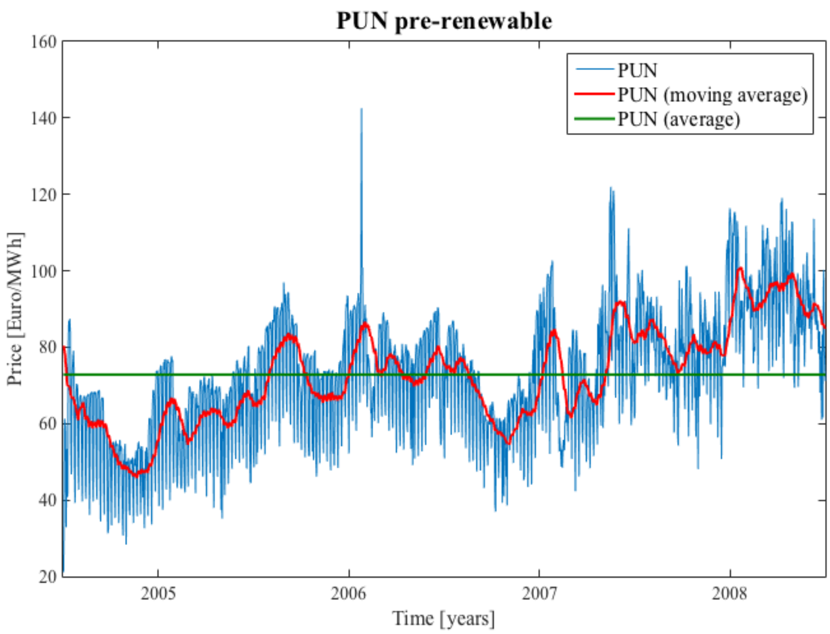

Figure 2-8: PUN daily time series in the pre-renewable period (2005 – 2008)

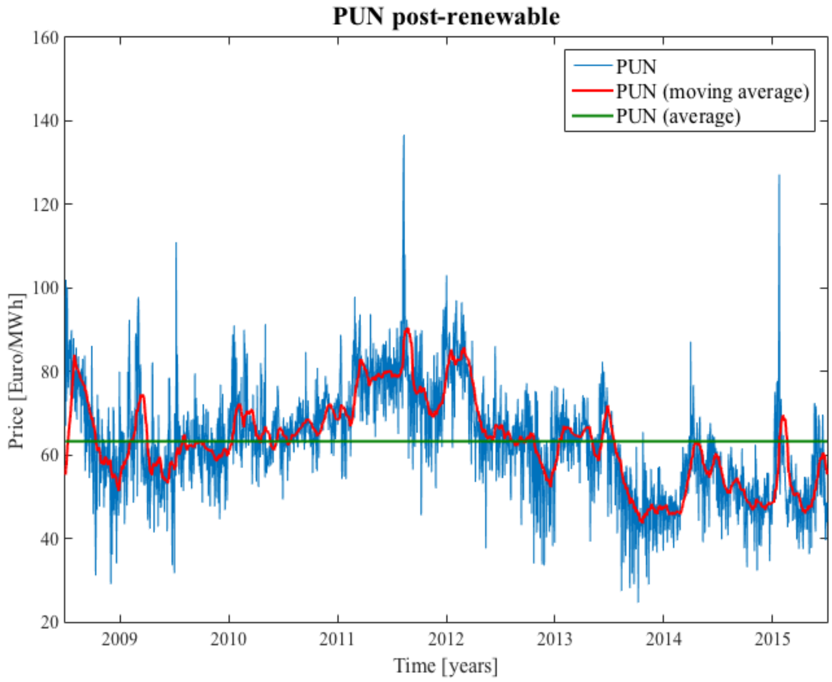

Figure 2-9: PUN daily time series in the post-renewable period (2009 – 2015)

Both the periods are characterized by high oscillation of the price, which decrease significantly during the weekend due to the lower energy demand. As explained in the previous chapter, we can note a significant decrease of the average price in the post-renewable period (63.3 Euro/MWh) w.r.t. the average price in the pre-renewable period (72.8 Euro/MWh). Starting from 2012 there was a further decrease of the price due to a percentage increase of the of total energy production from renewable sources.

3 Case study

3.1 Lake Como basin

The Lake Como, also called Lario, is a subalpine natural lake formed by the melting of the glacier of River Adda, its main tributary. With an area of 145 Km^2, it is the third largest Italian lake, after Lake Garda and Lake Maggiore and the first for perimeter length (about 185 Km). With a maximum depth of 410 m it is also one of the deepest lakes in Europe. In addition to the River Adda, many other rivers, mostly torrential, including Mera, Varrone and Pioverna, are tributaries to the lake. The only emissary of the lake is the River Adda, which flows from Lecco, through the Garlate and Olginate lakes, until it reaches the River Po.

Since 1946, following the construction of the Olginate dam, the Lake Como has become a regulated lake. Considering Olginate dam as closing section, the catchment of the River Adda has an area of 4762 Km^2, mostly extended in the Italian territory (about 90%), with the remaining 10% belonging to the Swiss territory, more precisely the territory of Val Bragaglia and Val Poschiavo (Figure 3-1).

The Adda River, after collecting the water of its catchment and the water diverted from the River Spoel, which naturally flows into the Danube catchment, flows into the Lake Como at Fuentes, with an average discharge of 88 m^3/s. From 1964, up to 90 Mm^3 per year are diverted from the River Spoel into the Lake of San Giacomo.

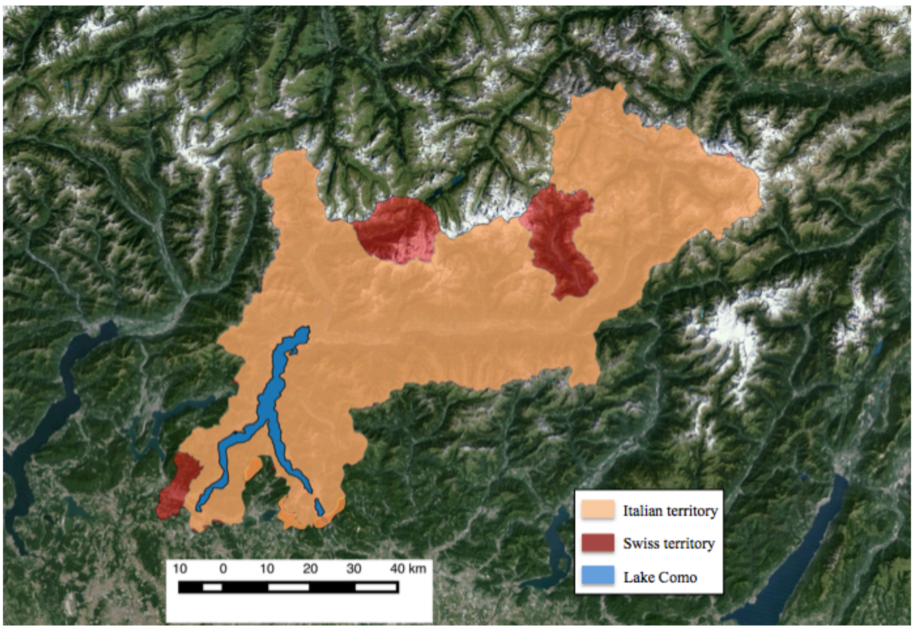

Figure 3-1: Map of the River Adda catchment. It is possible to distinguish the Italian part from the Swiss part of the basin

3.2 Hydropower system

Since the beginning of the last century, the territory of the River Adda basin, which is mostly mountainous and uneven, has been exploited for the construction of many artificial lakes and many plants for the hydroelectric production. This complex hydropower system, mostly owned by four of the main energy companies (A2A, Enel, Edison, Edipower), has a significant influence on the hydrology of the River Adda basin and consequentially on the inflow to the Lake Como. In fact, these seasonal reservoirs are able to move large volumes of water over time, altering the natural flow to the lake. The location and the features of the main reservoirs are shown in and in Figure 3-2 and in Table 3-1.

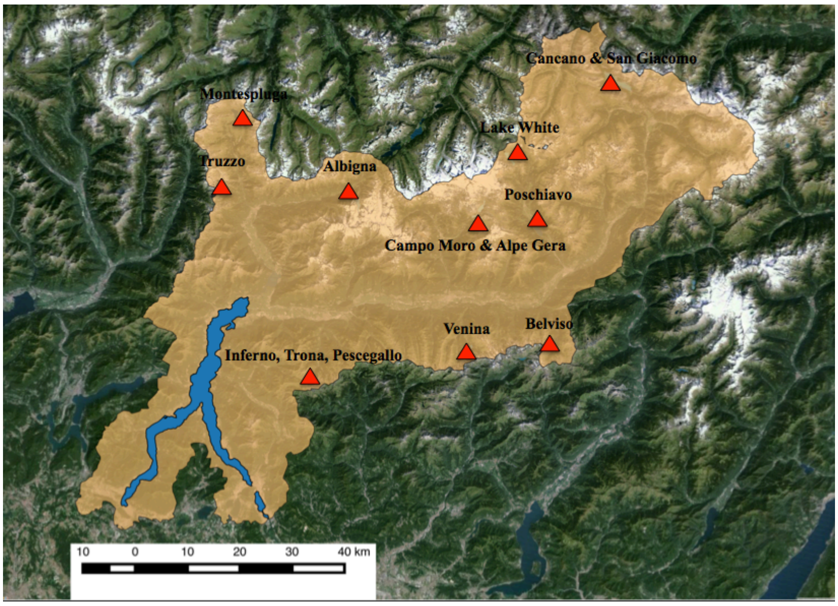

Figure 3-2: Map of the main reservoirs of the catchment

	Volume (Mm^3)	Altitude (m a.s.l.)	Natural Basin (Km^2)	Connected Basin (Km^2)	Company
Alpe Gera	68.1	2128	39.9	50.9	Enel
Campo Moro	10.8	1969	39.9	50.9	Enel
Inferno	4.2	2088	1.1	0.3	Enel
Trona	5.4	1805	2.6	11.5	Enel
Pescegallo	1.1	1863	0.9	1.0	Enel
San Giacomo	64.0	1952	18.7	322.3	A2A
Cancano	124.0	1902	36.0	322.3	A2A
Montespluga	32.6	1904	24.0	2.9	Edipower
Truzzo	20.0	2088	10.0	5.5	Edipower
Venina	11.2	1824	8.3	11.8	Edison
Belviso	50.1	1486	27.3	20.1	Edison
Albigna	69	2163	20.5	No data	EWZ
Lake White	18	2230	10.8	No data	Repower
Poschiavo	15.1	937	40.6	No data	Repower

Table 3-1: Table of the main features of the reservoirs of the catchment

3.2.1 A2A

The hydroelectric system of A2A (Figure 3-3) is spread over an area of 1000 Km^2 in Valtellina and produces annually about 1.7 billion of kWh with a dense hydropower network fed by two main contiguous reservoirs, located in the Fraele Valley: San Giacomo and Cancano (Figure 3-4, Figure 3-5). The first artificial lake, San Giacomo, has an altitude of 1951.5 m above sea level and a maximum capacity of 64 Mm^3. It was built in 1950 and collects the water diverted from the River Spoel and from the streams Gravia, Frodolfo, Alpe, Zebrù, Forcola, and Braulio, as well as the water coming from the natural course of the first part of the River Adda. Lake Cancano has an altitude of 1902 m above sea level and a maximum capacity of 123 Mm^3. It receives water directly from Lake San Giacomo and from the channel Viola. These two big artificial lakes feed the power plant of Premadio, which has a maximum capacity of 226 MW and a maximum allowable streamflow of 41.06 m^3/s. Downstream of the power plant of Premadio, the power plants of Grosio, Lovero and Stazzona are located in cascade.

Figure 3-3: A2A hydropower network – source: A2A

Figure 3-4: San Giacomo reservoir – source: ARPA

Figure 3-5: Cancano reservoir – source: A2A

3.2.2 Enel

The hydroelectric plants owned by Enel are located both on the right and on the left hydrgrafic side of River Adda. On the right side, in the territory of Val Malenco, the two main branches of the streams Mallero and Lanterna compose the hydrographic system. At the altitude of 1000m a.s.l. the stream Lanterna flows into the stream Mallero, which then flows into the river Adda, near the city of Sondrio. Two artificial lakes, Alpe Gera (Figure 3-8) and Campo Moro (Figure 3-9), are located along the course of the stream Lanterna, at the altitude of 2128 m and 1969 m above sea level respectively. Together they have a catchment area of 39.9 Km^2 and a connected area of 50.9 Km^2 and feed the power plant of Lanzada, which has an installed capacity of 188 MW. Alpe Gera, with a maximum storage of 68.1 Mm^3 is the bigger one; it is fed by the glacier Fellaria, through the stream Lanterna, and its release flows into the lake Campo Moro, which has a maximum storage of 10.8 Mm^3 (Figure 3-6).

On the left hydrografic side of River Adda, in the territory of Val Gerola, there are three small reservoirs, Pescegallo, Inferno e Trona, which feed the power plant of Trona and the main one of Gerola Alta, which has an installed capacity of 13.8 MW. These reservoirs have a small catchment and represent a minor part of the Enel network in Valtellina. The Lake Pescegallo is located at an altitude of 1863 m and has a maximum storage of only 1.1 Mm^3. Its natural catchment and the connected basin don't reach together the area of 2 Km^2. The Lake Inferno has a maximum storage of 4.17 Mm^3 and an altitude of 2088 m. The Lake Trona, located 1802 m above sea level, has a maximum storage of 5.35 Mm^3 and presents a catchment area of 2.62 Km^2 and a connected basin of 11.5 Km^2 (Figure 3-7).

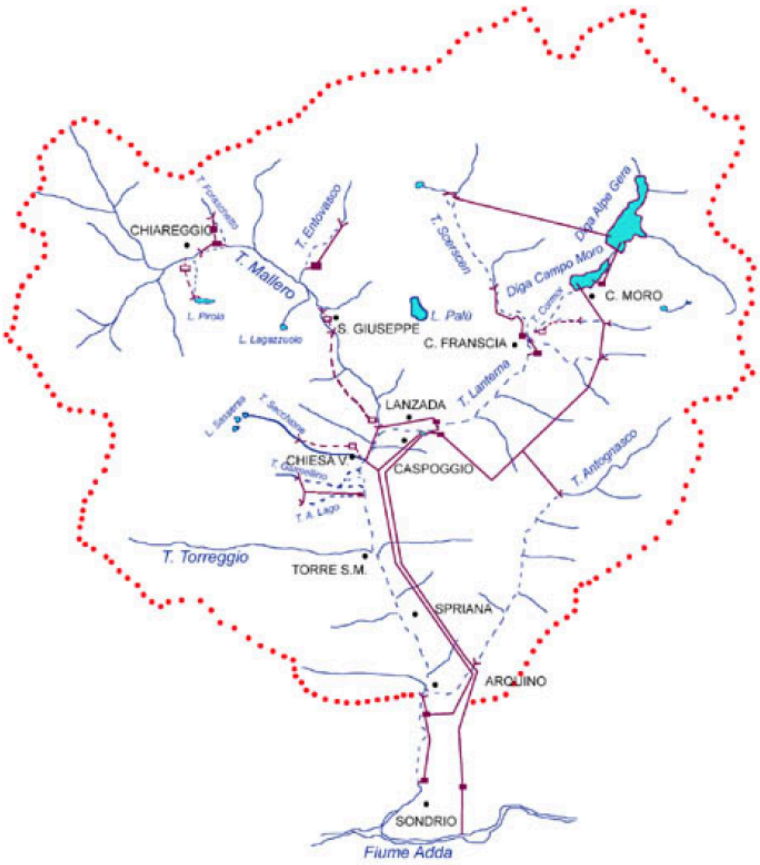

Figure 3-6: Enel hydropower network in Val Malenco – source: Enel

Figure 3-7: Enel hydropower network in Val Gerola – source: Enel

Figure 3-8: Alpe Gera reservoirs – source: Enel

Figure 3-9: Campo Moro reservoirs – source: Enel

3.2.3 Edison

The hydropower network of Edison in the territory of Valtellina is located on the left hydrografic side of the River Adda and consists in two hydraulic links: the link Venina-Armisa (Figure 3-10) and the link Ganda-Belviso (Figure 3-11). The Lake Venina is located at an altitude of 1824 m above sea level. It's mainly fed by the Venina River and it has a maximum storage of 11.2 Mm^3. It has a natural catchment area of 8.3 Km^2 and a connected basin of 11.8 Km^2. The Lake Venina feeds the Venina power plant, which has an installed capacity of 67 MW and a streamflow concession of 25.3 m^3/s.

The lake Belviso, born after the construction of the Frera dam, has an altitude of 1486 m above sea level and it's fed by the River Belviso. This big reservoir has a maximum storage of 50.1 Mm^3, a catchment area of 27.3 Km^2 and a connected basin of 20.1 Km^2. With its release, the Lake Belviso feeds the power plants of Ganda and Belviso, which have both an installed capacity of 66 MW.

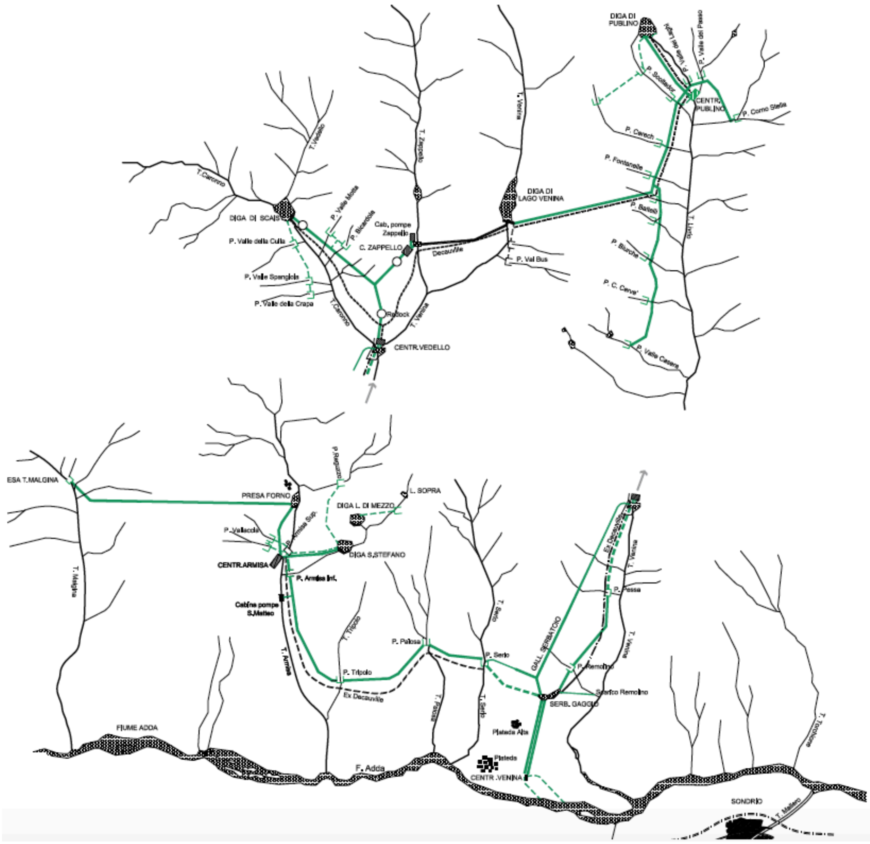

Figure 3-10: Edison hydropower network in the area of lake Venina – source: Edison

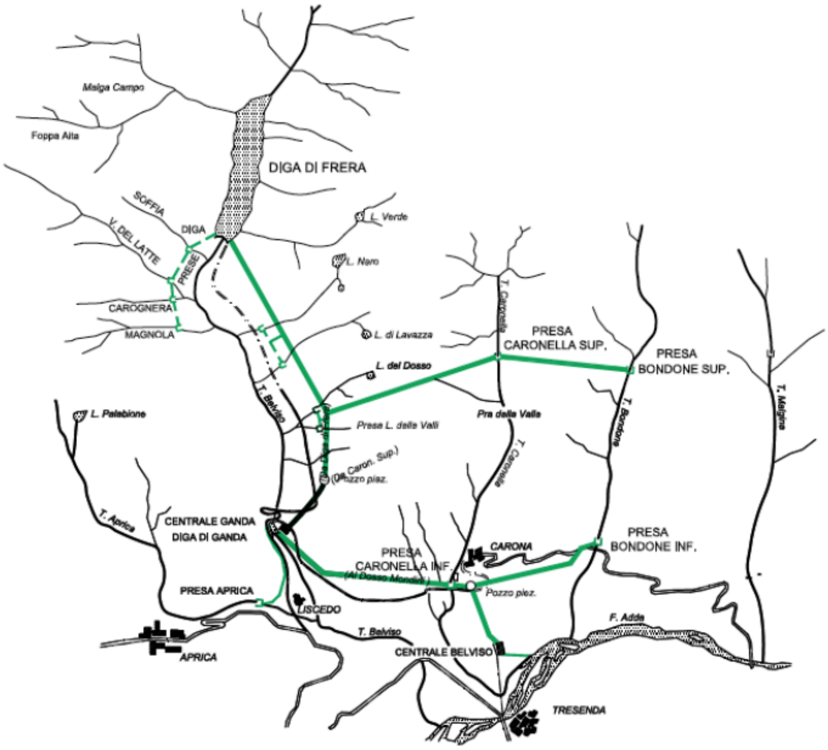

Figure 3-11: Edison hydropower network in the area of lake Belviso – source: Edison

3.2.4 Edipower

The Edipower hydroelectric network consists in 8 power plants in the territory of Valchiavenna and 4 power plants in the province of Como, for a total installed capacity of 382 MW.
The power plants and the reservoirs of Valchiavenna (Figure 3-12) are located along the rivers Liro and Mera. River Liro's source is located at an altitude of over 3000 m above sea level near the Spluga pass. This river, after 25 km, flows into the River Mera, near the city of Chiavenna. The River Mera is born in Swiss territory at an altitude of over 2800 m above sea level and it reaches the Italian territory in Castesegna. Due to the morphologic and climatic's characteristics of Liro and Mera valleys, which extend to the north of the Lake Como, the territory of Valchiavenna is characterized by intense and frequent precipitation events.
The Lake Montespluga collects the water of the River Liro through two dams, Cardanello and Stuetta. This lake has a maximum storage of 32.6 Mm^3 and an altitude of 1903.5 and feeds the power plant of Isolato Spluga, which is located in the municipality of Madesimo. The Lake Montespluga has a catchment area of 24 Km^2 and a connected basin if 2.85 Km^2.
The Lake Truzzo is located at the altitude of 2088 m a.s.l. and it has a maximum storage of 20 Mm^3. It has a catchment area of 10 Km^2 and a connected basin of 5.5 Km^2 and feeds the power plant of San Bernando, which is located in the province of Sondrio.
Downstream these two reservoirs, the biggest power plant is the one of Mese, which has an installed capacity of 177 MW.

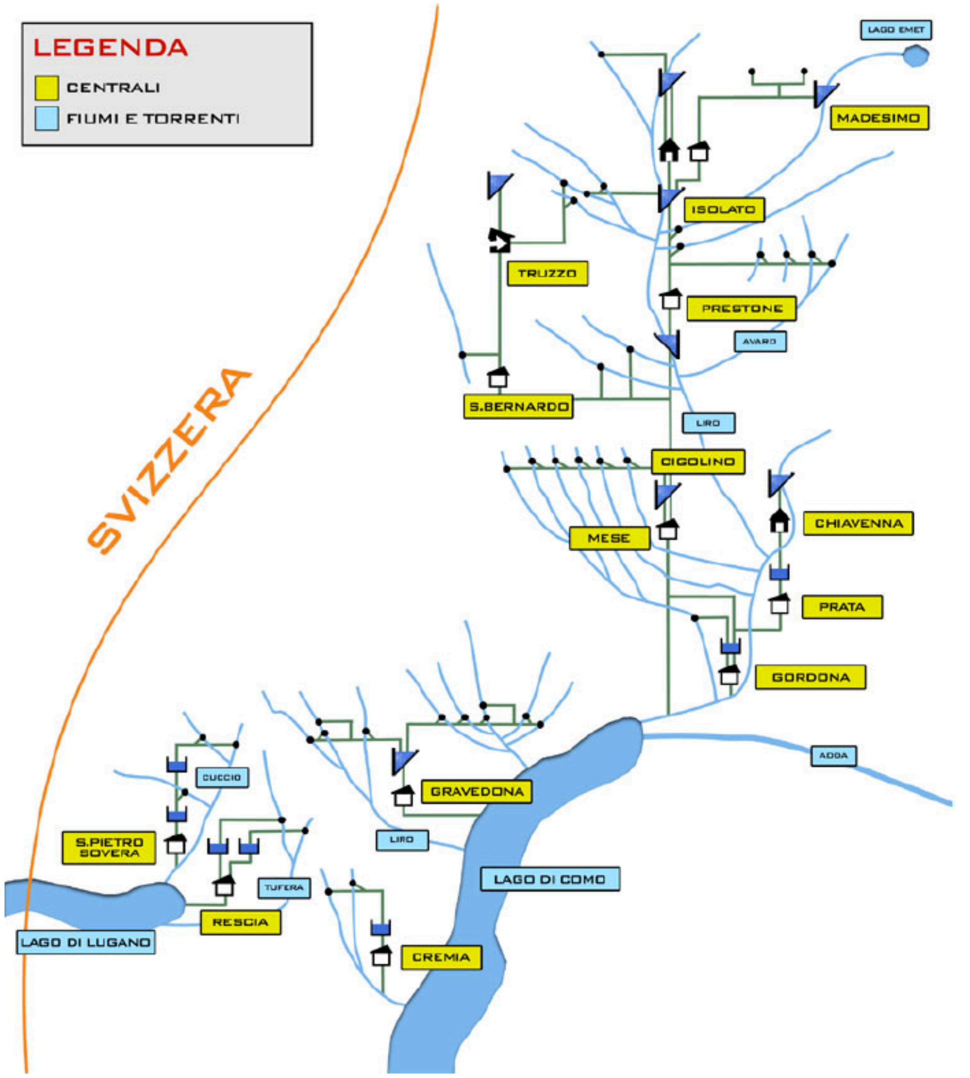

Figure 3-12: Edipower hydropower network in Valchiavenna – source: Edipower

3.2.5 Repower

The hydropower network belonging to Repower is located in Switzerland, more precisely in the territory of the Val Poschiavo (Figure 3-13).
After the construction of the dams of Scala and Arlas, also called North dam and South dam, the lakes of Bernina has been merged into a lake, called Lake White. The Lake White is located at an altitude of 2230 m above sea level between the municipalities of Poschiavo and Pontresina. It has maximum storage of 18 Mm^3 and it can be considered a tipical seasonal reservoir. It receives water from its own catchment and, through a pumping plant, from the Lake Palù, which is located 300 m downstream of the lake. The Lake White and the Lake Palù feed three power plants: Palù, with an installed capacity of 10 MW, Cavaglia, with an installed capacity of 7 MW and Robbia, the biggest one, with an installed capacity of 27 MW. The

water, exploited from these power plants, flows, through the River Poschiavino, into the Lake Poschiavo.
The Lake Poschiavo is a natural lake with a maximum storage of 15.1 Mm^3. This lake feeds the power plant of Campocologno, which has an installed capacity of 45 MW and a streamflow concession of 13 m^3/s.

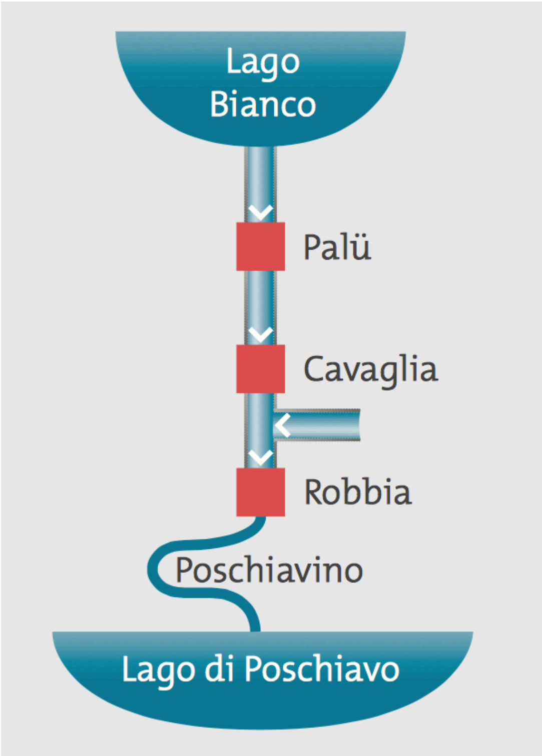

Figure 3-13: Repower hydropower network in Val Poschiavo – source: Repower

3.2.6 EWZ

The main reservoir belonging to EWZ is the Lake Albigna (Figure 3-14), which is located on the southwest side of the Bregaglia valley, in the municipality of Vicosoprano. It has a maximum storage of 69 Mm^3 and an altitude of 2163 m above sea level. Its catchment area is 20.5 Km^2. This lake feeds the power plant of Lobbia, which as an installed capacity of 95 MW.

Figure 3-14: Albigna reservoir – source: EWZ

3.2.7 Simplifications and notes

Concerning the hydrological model, in this thesis we'll take into account all the hydropower reservoirs located in the River Adda basin, with the exception of the Lake Pirola and the Lake Palu, due to scarcity of data.
Regarding the implementation of the hydroelectric operators' behavioural model, all the analysis will be focused on the reservoirs owned by Enel (e.g., Alpe Gera and Campo Moro) and A2A (e.g., San Giacomo and Cancano), due to lack of information for the others.
Nevertheless these reservoirs account for more than 50% of the total water storage of the Lake Como catchment.

4 Hydrological model (Topkapi-ETH)

4.1 Setup

As explained in chapter 2.1, the distributed physical-based model Topkapi-ETH requires time series of air temperature, cloud cover trasmissivity and precipitation for each grid cell at the temporal and spatial resolution selected for the model simulation, as well as a series of spatial inputs, which define the main characteristics of the catchment. In order to obtain a good compromise between reasonable computational time and an accurate representation of the complexity of the system, we implement the model using a spatial grid of 250 m^2 and a daily temporal resolution.
The pre-processing phase, which is the process of selection and definition of the model inputs, is a crucial step in the implementation of the distributed physical based hydrological models. In fact, the goodness of the simulation phase outputs depends mainly on the accuracy of the model inputs. We describe the process of selection of the hydrometeorological data (air temperature, cloud cover trasmissivity and precipitation) in chapter 4.1.1. Chapter 4.1.2 describes, instead, the main spatial inputs.

4.1.1 Hydrometeorological data

Different measuring stations belonging to ARPA (Regional Agency for the Protection of the Environment) are distributed throughout the Lake Como catchment and record temperature, precipitation. We selected the station to be included in the model based on three criteria:

- The selected stations have to provide good quality time series (e.g., few missing data)
- The selected stations have to be uniformly distributed throughout the catchment.
- The selected stations have to provide data over the longest common time period.

Table 4-1 shows temperature and precipitation selected stations with some statistics about the data quality. A single station, located slightly outside the catchment, at the Samedan airport, provides instead the only available information on cloud cover trasmissivity.
The selected time period, used to calibrate and validate the model (see chapter 4.2), is 2003-2013 (11 years).

Temperature				
Name	Altitude [m a.s.l.]	Data quality analysis (missing data)		
		%	Max consecutive days (d)	Mean consecutive days (d)
Lecco	214	1.4	8	3.6
Colico	229	2.7	28	5.5
Bormio	1225	3.0	28	7.6
Tirano	439	3.2	106	12.7
Precipitation				
Name	Altitude [m a.s.l.]	Data quality analysis (missing data)		
		%	Max consecutive days (d)	Mean consecutive days (d)
Cancano	1948	3.4	48	6.4
S.Caterina Valfurva	1730	3.9	47	5.1
Alpe Entova	1905	2.5	97	11.3
Samolaco	206	9.6	103	35.0
Bormio	1225	1.2	42	7.7
Colico	229	2.8	28	5.6
Oga S. Colombano	2300	6.6	58	8.7
Aprica	1950	4.0	55	9.6

Table 4-1: Temperature and precipitation stations selected as inputs of the model

4.1.2 Spatial data

Digital Elevation Model

The Digital Elevation Model (Figure 4-1) is obtained from the Shuttle Radar Topography Mission, a space mission coordinated by National Aeronautics and Space Administration and National Geospatial - Intelligence Agency. A DEM is required in Topkapi-ETH to extract information about the catchment area, the flow direction, and the river network.

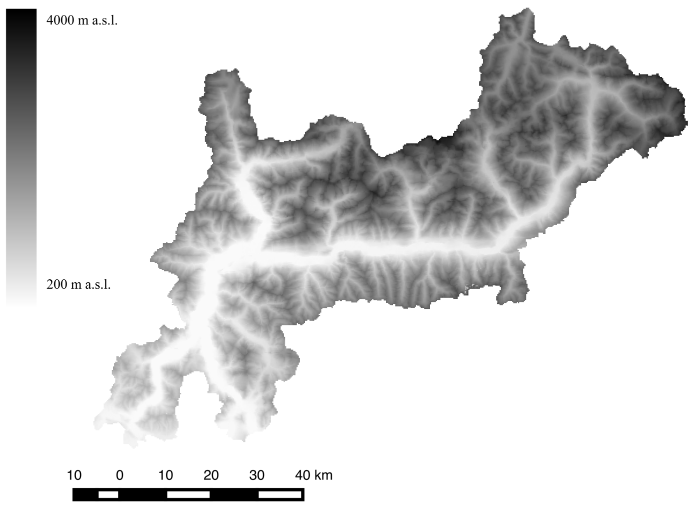

Figure 4-1: Digital Elevation Model of the catchment

Soil Map

Since the Lake Como basin extends over two countries, Italy and Switzerland, the information concerning soil is obtained from two different sources and then merged together using a Geographical Information System (GIS). For the Italian part of the catchment, the soil map is provided by the local ARPA. For the Swiss part we retrieve the soil information from the Swiss Federal Agriculture Office (Bundesamt für Landwirtschaft). As shown in Figure 4-2, a sandy-loam soil characterizes almost the entire Italian part of the basin. The Swiss part is instead characterized by a clay/clay-loam soil. Parameters regarding thickness and hydraulic properties are associated to each soil class.

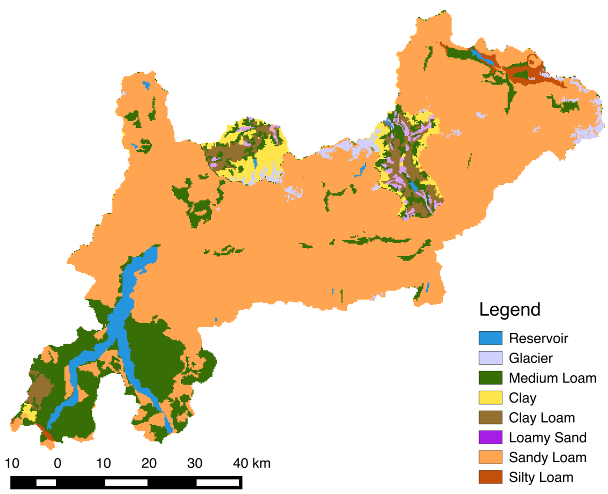

Figure 4-2: Soil Type map

Land Cover Map

Also the information regarding the land cover is obtained from two different sources. For the Italian part of the basin, we use the map Destinazione d'Uso dei Suoli Agricoli e Forestali (DUSAF), a product developed by ARPA. For the Swiss part, the only available map is the Corine Land Cover, a European land cover map less detailed than DUSAF (Figure 4-3).

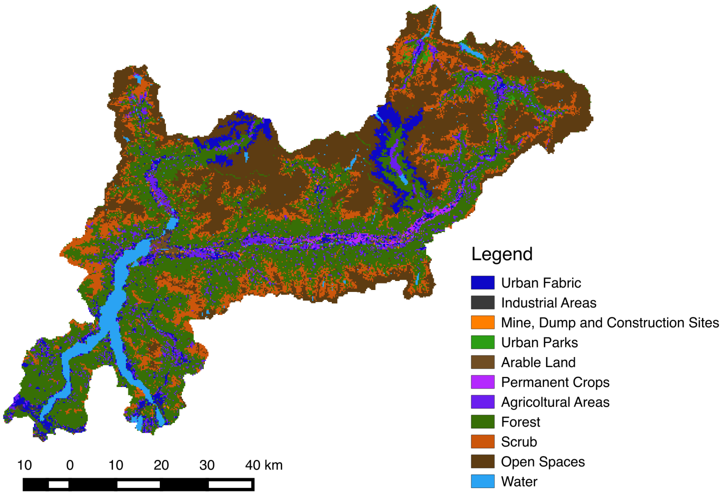

Figure 4-3: Land Cover map

Glaciers Map

The information regarding the Italian glaciers is provided by the local ARPA. Since there is no available information on the glaciers' ice thickness, this data is estimated from the area, with an empirical formula and assuming a uniform ice thickness, as follows [Fatichi et al., 2013; Farinotti et al., 2009]

$$h_{ice} = 33A^{0.36}$$

where A[km^2] is the area of the single glacier and h_{ice}[m] represents its ice thickness.
A distributed glaciers' ice thickness map is instead available for the Swiss part of the basin [Huss and Farinotti, 2012; Fisher et al., 2014].
The two maps are merged together within a GIS (Figure 4-4).

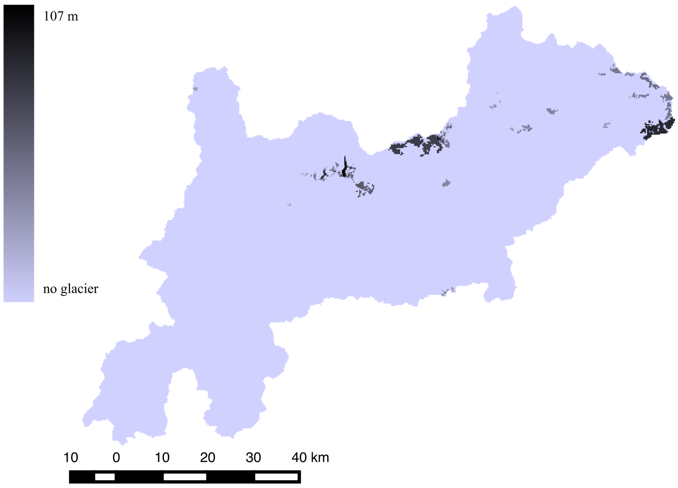

Figure 4-4: Glaciers Depth map

Reservoirs Map

Figure 4-5 shows the hydropower reservoirs included in the analysis as well as the Lake Como. In order to simulate the reservoirs dynamic, Topkapi-ETH allows choosing from different reservoir operating rules, defined separately for each artificial lake. Besides the location and the spatial extent of each reservoir, Topkapi-ETH requires other inputs that define the main characteristics of the lakes. The main reservoir simulation modes are explained in chapter 6.

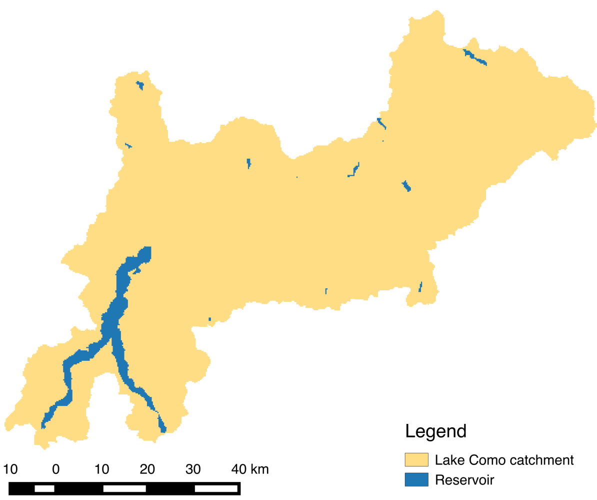

Figure 4-5: Reservoirs map

Groundwater Depth Map

The groundwater depth map is an optional input and defines the groundwater aquifer thickness for each grid cell. Topkapi-ETH is able to simulate the groundwater flow with an approach described in Liu et al. [2005], which take into account the percolation to deep soil layers and groundwater flows. In this thesis, we define two groundwater classes (Figure 4-6):

- 8 meters deep, at lower altitudes along the river network
- 2 meters deep, for the rest of the catchment

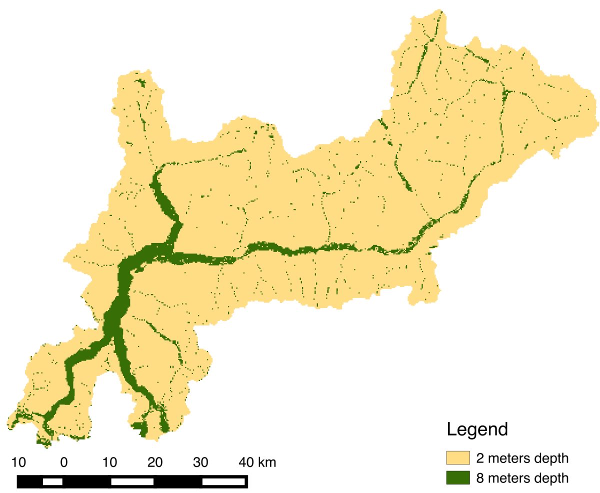

Figure 4-6: Groundwater Depth map

Thiessen Polygons for Temperature, Precipitation and Cloud Cover Trasmissivity

In order to define temperature, precipitation and cloud cover trasmissivity values for each grid cell, Topkapi-ETH allows to provide 1D time series of point measurements or 2D maps covering the entire catchment. In both cases, data has to be provided for each simulation time step. As explained in chapter x, in this thesis we use time series provided by different measuring station, which has to be transformed from point to maps, computing the Thiessen polygons in a GIS environment.
Figure 4-7 and Figure 4-8 show the maps obtained for temperature and precipitation. For cloud cover trasmissivity, we consider only one Thiessen polygon for the entire catchment because we have only one station that provides data.

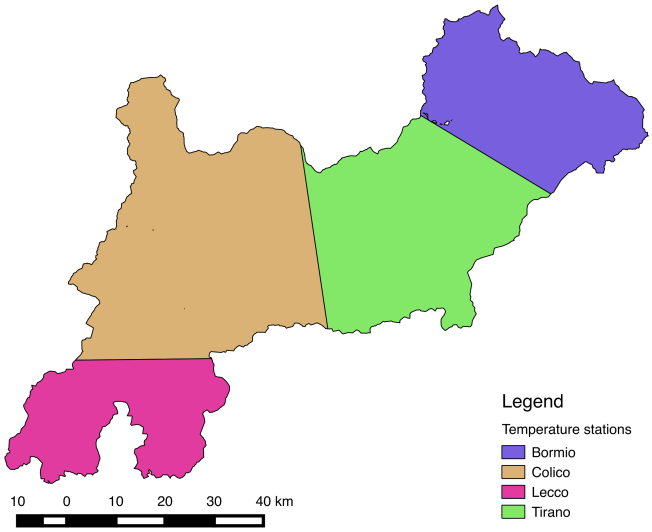

Figure 4-7: Temperature Thiessen Polygon map

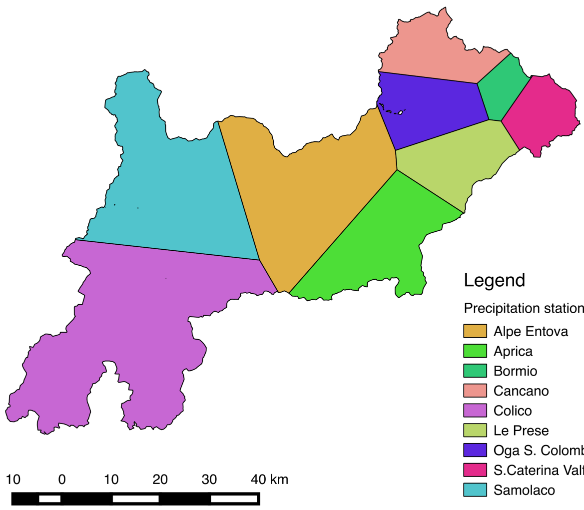

Figure 4-8: Precipitation Thiessen Polygon map

Precipitation Correction Maps

In order to increase the spatial accuracy of precipitation data, a monthly correction factor is applied on the precipitation time series, through the definition of correction maps with a spatial resolution of 5 km^2. These maps, one for each month, contain a multiplicative correction factor for each grid cell, computed starting from a precipitation grid dataset, result of a trans-national analysis that has been carried out collecting information from precipitation gauges over the Alpine area in seven countries (Italy, Switzerland, Austria, Germany, France, Slovenia, and Croatia) with approximately 5500 measurements per day from 1971 to 2008 [Isotta et al., 2014].

4.2 Calibration and Validation

Even though Topkapi-ETH is a physical based model, the process of calibration constitutes a substantial step in order to obtain good results in simulation. In fact, according to Beven [2012], estimating the parameters of the model by measurements or prior estimation is, in general, very difficult. The process of calibration consists in the optimisation of the parameters values by comparing the results of repeated simulation with the available observed data of the catchment response.
Measurements of flow In the Lake Como catchment are only available at the section of Fuentes. Here the flow, estimated from level's observation with an empirical relation, is strictly related to the behaviour of the alpine reservoirs, which shift high volumes of water in space and time, altering the natural flow significantly.
Since we don't have enough data and information to reproduce the operating rules of all the reservoirs present in the basin, we calibrate and validate the model on the inflow of the main equivalent reservoirs of A2A and Enel companies (Figure 4-9):

- *San Giacomo* and *Cancano* reservoirs are merged together forming the A2A equivalent reservoir.
- *Alpe Gera* and *Campo Moro* reservoirs are merged together forming the Enel equivalent reservoir.

These reservoirs, which have a natural basin, account for more then 50% of the total water storage of the Lake Como catchment and they are used, in this thesis, to implement reservoirs behavioural models (see chapter 5).

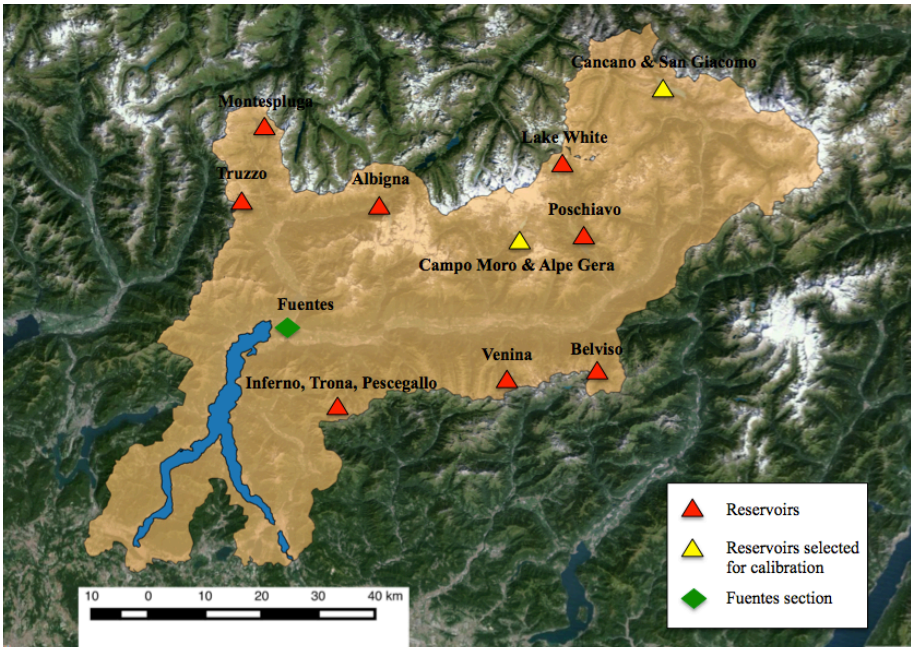

Figure 4-9: Lake Como catchment with all reservoirs, Lake Como and the section of Fuentes

The inflow data, used for the calibration and validation phases, has been reconstructed through mass balance starting from storage and release data, provided by ARPA.

The calibration of Topkapi-ETH is performed manually, starting from literature values of the parameters related to soil and snow properties: since all the parameters of the model have a physical meaning, the calibration consists in adjusting these parameters, moving in a range of acceptable values, to improve the performances of the model with regard to the available reservoirs inflow time series. More precisely, we adjust the following parameters:

Snow/Ice Parameters

- **Alfa$_{max}$:** it represents the maximum fresh snow albedo according with Brock et al. [2000].
- **R$_d$:** it represents an empirical albedo decline factor according with Brock et al. [2000]
- **AlbedoReset:** it represents the solid precipitation threshold to reset snow albedo. If the solid precipitation is grater than this threshold, the snow albedo is set to Alfa$_{max}$.
- **AlbedoGlacier:** it represents a lumped value of ice albedo. This parameter is only used when glaciers are present in the catchment a no ground albedo map is provided.
- **PrecSF:** it represents the threshold air temperature to distinguish between liquid and solid precipitation.
- **Ttsnow**: it represents the threshold air temperature for melt onset at grid cell level.

- **MeltOnsetTimesteps**, **MeltOnsetTemp:** MeltOnsetTimesteps represents the number of simulation time steps (integer value) at which the air temperature defined by MeltOnsetTemp needs to be exceeded by the mean elevation band (100 m interval) air temperature to allow general melt onset.

Soil Parameters

- **Soil Depth:** it represents the soil thickness of the two layers defined in Topkapi-ETH.
- **Residual water content ratio (ThetaR) and water content ratio at saturation (ThetaS):** they represent the water content characteristics of the two soil layers.
- **Horizontal (KsH) and vertical (KsV) hydraulic conductivity**: they are a measure of saturated soil ability to transmit water when subjected to a hydraulic gradient. These parameters vary within a wide range of orders of magnitude, depending on the soil type.

The calibration performance is assessed using three indices: the coefficient of determination (R^2), the root of the mean square error ($RMSE$), and Kling-Gupta Efficiency (KGE).

R^2 represents the portion of the total variance of the observed data that can be explained from the model:

$$R^2 = 1 - \frac{var(y_{obs} - y_{sim})}{var(y_{obs})}$$

where y_{obs} and y_{sim} are the observed and the simulated time series respectively.
This metric is very sensitive to outliers and insensitive to additive and proportional differences between model simulations and observations. Therefore, in case of systematic underestimation or overestimation of the streamflow, if the model can follow the observed data during extreme events, the value of R^2 will be high, obscuring the true relationship between the model-simulated and observed data [Legates and McCabe, 1999].

$RMSE$ represents the standard deviation of the difference between observed and predicted values and it is widely used in hydrological modeling [Legates and McCabe, 1999]:

$$RMSE = \sqrt{\frac{\sum_{t=1}^{N}(y_{obs,t} - y_{sim,t})^2}{N}}$$

where $y_{obs,t}$ and $y_{sim,t}$ are the observed and simulated values at time t respectively and N represents the length of the time series.

KGE is an alternative measure of performance for hydrological models which aims to overcome the traditional problems associated with calibration, for instance variability underestimation and low sensitivity to proportional and additive variations [Gupta et al., 2009]:

$$\alpha = \frac{\sigma_{sim}}{\sigma_{obs}}, \beta = \frac{\mu_{sim}}{\mu_{obs}}, r = \sqrt{R^2}$$

$$ED = \sqrt{(r-1)^2 + (\alpha-1)^2 + (\beta-1)^2}$$

$$KGE = 1 - ED$$

where σ_{obs} and σ_{sim} are the observed and simulated standard deviation of the time series and μ_{obs} and μ_{sim} are the two means.

We calibrate the model on the period 2003-2009, considering 3 years of warm up, and validate it on the period 2010-2013. The results of the calibration are shown in Figure 4-10, Figure 4-11, Figure 4-12, Figure 4-13.

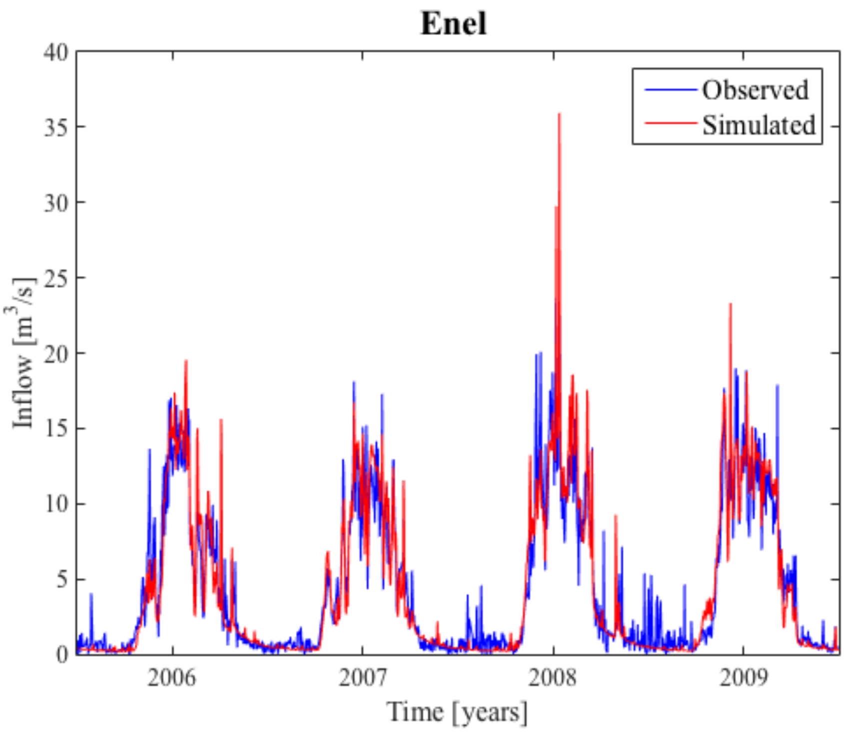

Figure 4-10: Comparison between observed and simulated inflow of Enel reservoir

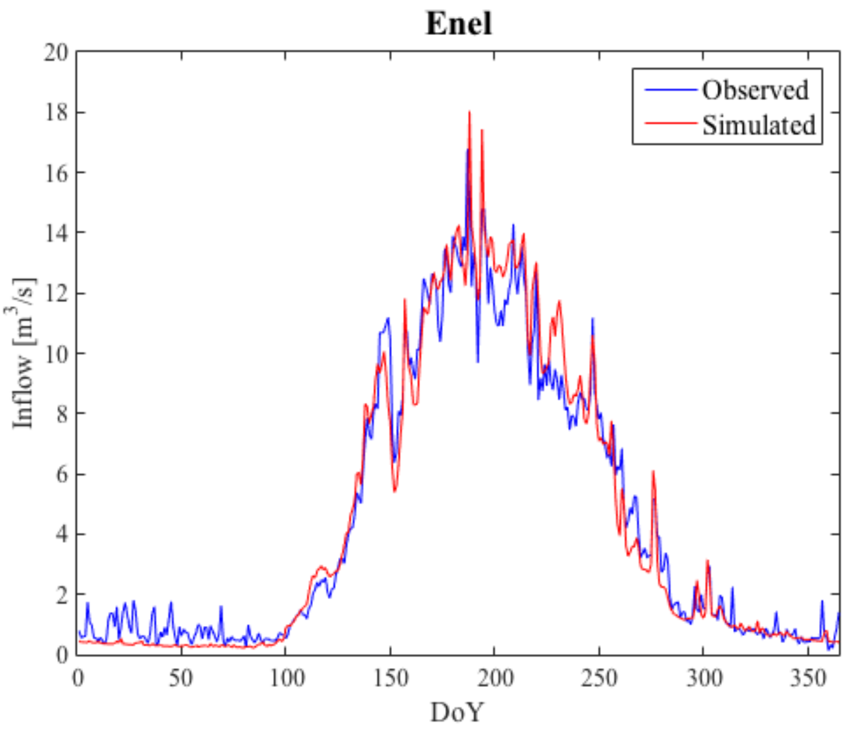

Figure 4-11: Comparison between observed and simulated average inflow per day of the year (DoY) of Enel reservoir

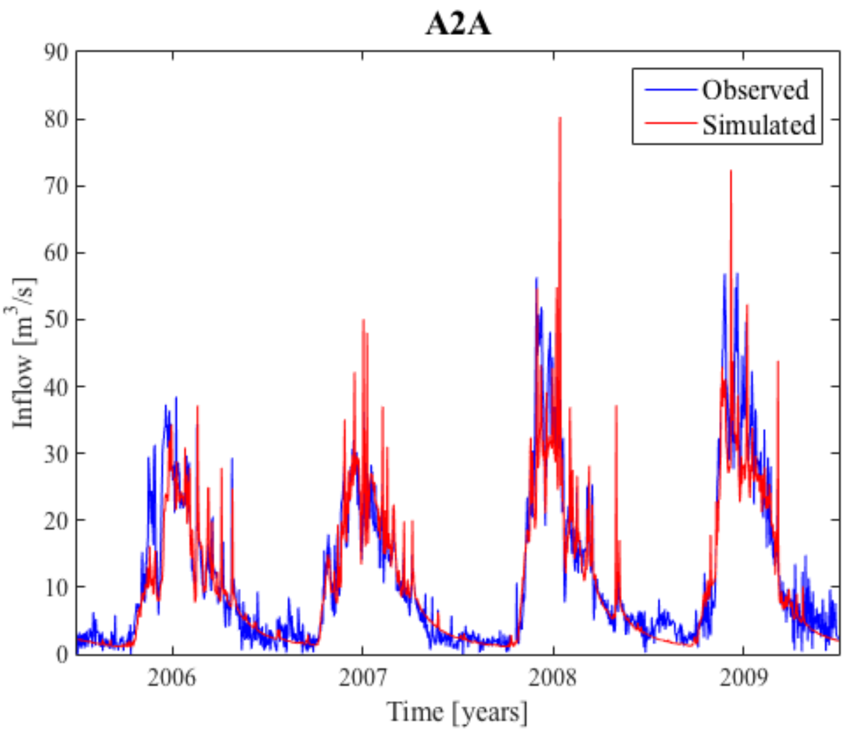

Figure 4-12: Comparison between observed and simulated inflow of A2A reservoir

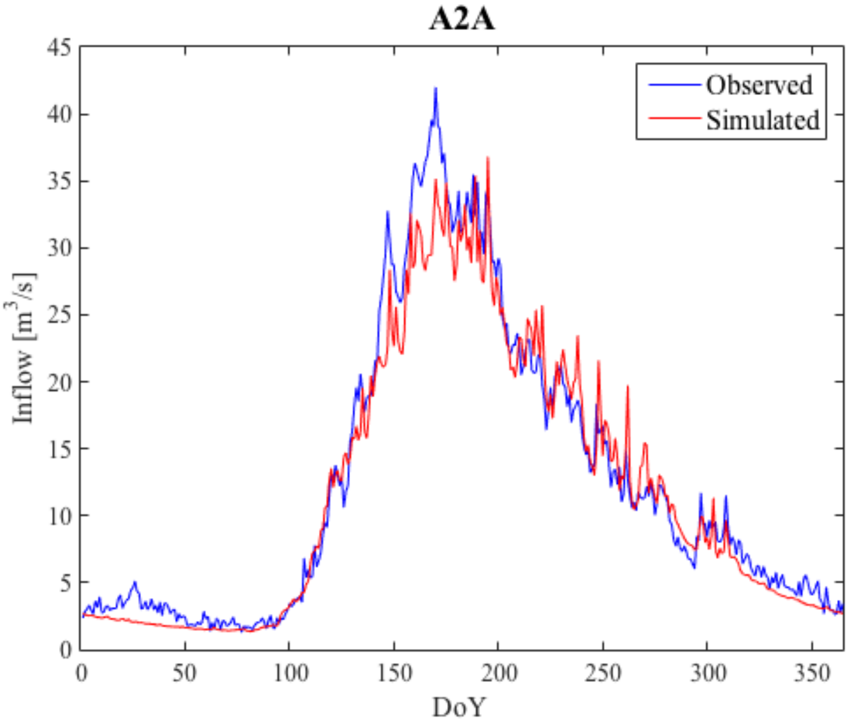

Figure 4-13: Comparison between observed and simulated average inflow per day of the year (DoY) of A2A reservoir

Table 4-2 shows the results of the calibration and validations phases in terms of the metrics selected.

Metrics	Enel		A2A	
	Calibration	Validation	Calibration	Validation
R^2 [-]	0.89	0.81	0.84	0.81
RMSE [m^3/s]	1.62	2.20	4.78	5.30
KGE [-]	0.92	0.84	0.85	0.88

Table 4-2: Results of calibration and validation phases

Considering the spatial resolution of 250 m^2 and the daily temporal resolution of the model, the indices values obtained in calibration are very satisfactory for both the reservoirs. Although the model has a slightly decrease of performance in validation, the values of the metrics remain widely acceptable.

As shown in Figure 4-11 and Figure 4-13, the model is able to reproduce the observed inflow annual pattern very well, capturing with high precision the snowmelt dynamics. Analysing Figure 4-10 and Figure 4-12 in more detail, we can notice that, on the contrary, the model is not able to capture the observed winter fluctuations: this is mainly due to two different factors, one related to low spatial and temporal resolution with respect to the small catchments of the reservoirs, and one related to possible measuring errors in the storage and release observed data, used to reconstruct the inflow by mass balance.

The performances of the model at Fuentes, the only section in which we have measurements of the flow, are shown in Figure 4-14. We can see that the model underestimates, in almost all the simulation years, the flow observed in the spring time, when the snow-melt occurs. This is mainly due to the model underestimation of the snowpack in the winter period as we can see from the comparison between the maps of Snow Water Equivalent (SWE) produced by the model and those produced by ARPA for some days of the year 2011. Figure 4-15 shows the comparison between the observed and simulated flow at Fuentes in the year 2011. Figure 4-16 shows the maps of the differences between the SWE estimated by Topkapi-ETH and the SWE estimated by ARPA in two different days of the year 2011. The underestimation of Topkapi-ETH occurs in almost all the catchment.

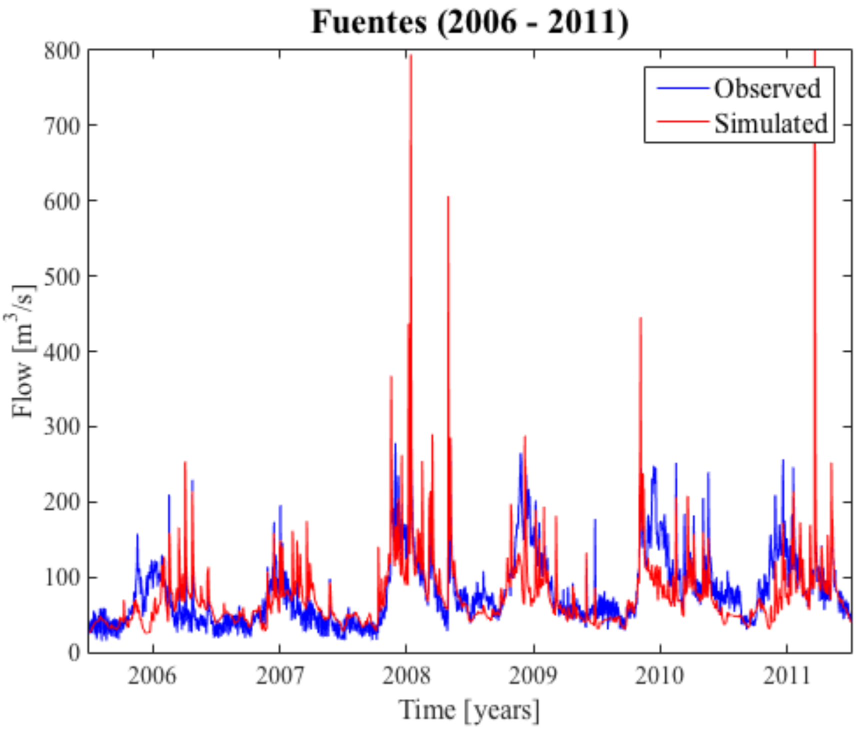

Figure 4-14: Comparison between observed and simulated flow at Fuentes

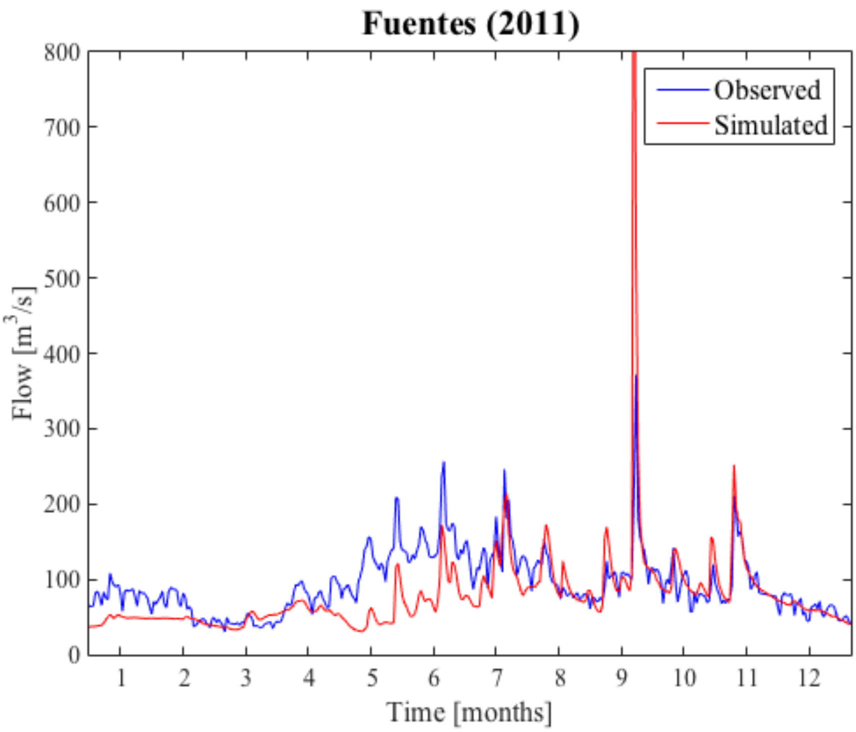

Figure 4-15: Comparison between observed and simulated flow at Fuentes in the year 2011

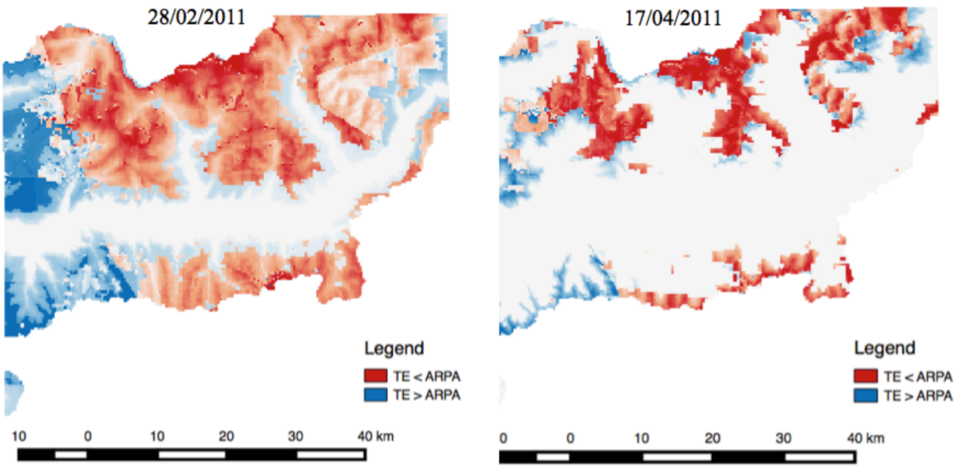

Figure 4-16: Maps of the differences between the SWE estimated by Topkapi-ETH and the SWE estimated by ARPA

5 Hydropower behavioural model

As described in chapter 2.2, we implement an implicit, or optimisation based, behavioural model. We suppose that hydropower companies are rational agents, who maximize the total revenue obtained from the sale of electricity produced by the turbines downstream from the reservoirs.
Since the Alpine hydropower systems considered in this thesis are composed by a single reservoir, which feeds more than one power plant, each with its own maximum flow and energy coefficient, we model the cascade of power plants by means of an equivalent plant with a capacity equal to the smallest plant capacity and an energy coefficient equal to the sum of the energy coefficients of all plants [Anghileri et al., 2013]
In our behavioural model, the management of the hydropower system consists in releasing the maximum flow during the most profitable hours of the day. Therefore the decision variable is the number of operating hours of the equivalent power plant, (instead of the more common release from the reservoir). In other words, the optimal control problem of the day t consists in defining for how many hours the decision maker has to release the maximum flow of the turbine in order to maximize the revenue.
However, the reservoir release and the number of operating hours are univocally related:

$$h_t = \frac{r_t}{Q_{max}^T} \cdot 24$$

where h_t $[hours]$ is the number of operating hours, r_t $[m^3/s]$ the daily average release from the reservoir and Q_{max}^T $[m^3/s]$ the maximum flow of the turbine.
We underline that in reality r is not released over 24 hours, but Q_{max}^T is released for h hours. Therefore the energy produced for each operating hour is always the same:

$$G = k \cdot Q_{max}^T \cdot 3600$$

where G $[KWh]$ is the energy produced for each operating hour, k $[KWh/m^3]$ is the energy coefficient of the equivalent power plant and Q_{max}^T $[m^3/s]$ is the maximum flow of the turbine.
The optimal decision depends also on the price the energy assumes every hour of the day. In order to calculate the revenue at each time step, we generate, starting from an hourly prices time series on the period 2005-2015 (see chapter 2.3.2), a price matrix, which provide for every day of the anthropic year (a non-leap year which start on Monday and has 364 days), the mean energy price, cumulated from the lowest to the highest profitable hour (Figure 5-1). The anthropic time allows keeping distinct weekdays from weekends, when the price decreases significantly due to the lower energy demand, in order to obtain a realistic average price. More precisely, the prices of the weekdays are mediated with a moving average of

amplitude 5 days and the prices of the weekends are mediated without moving average.
With the same procedure, we calculate the price matrix over the period 2005-2008, which identifies the pre-renewable scenario (Figure 5-2) and over the period 2009-2015, which identifies the post-renewable scenario (Figure 5-3).

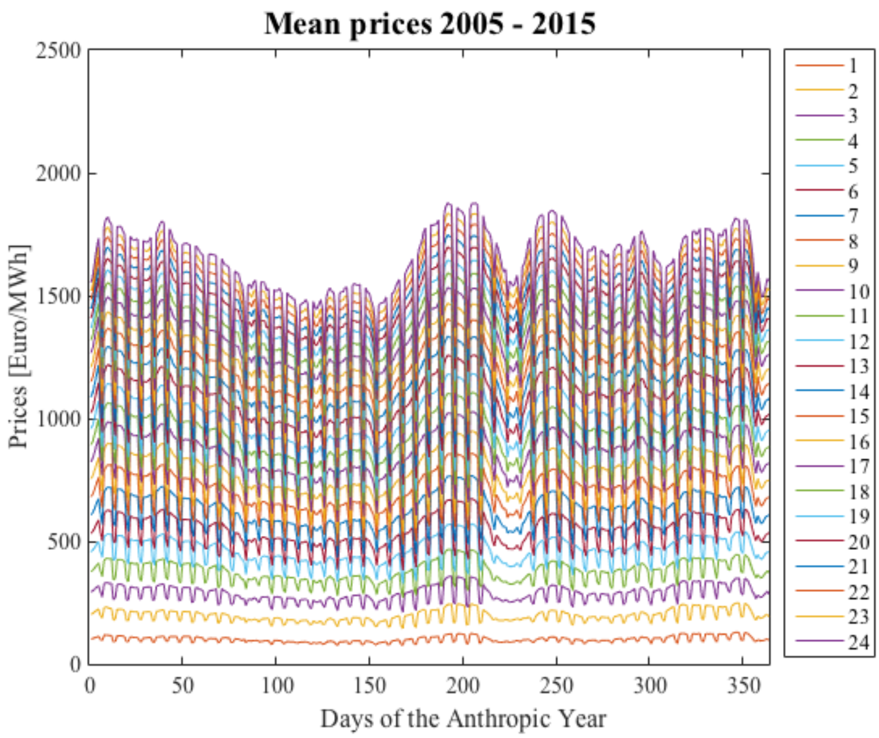

Figure 5-1: Mean energy prices on the period 2005 – 2015 cumulated from the lowest to the highest profitable hours

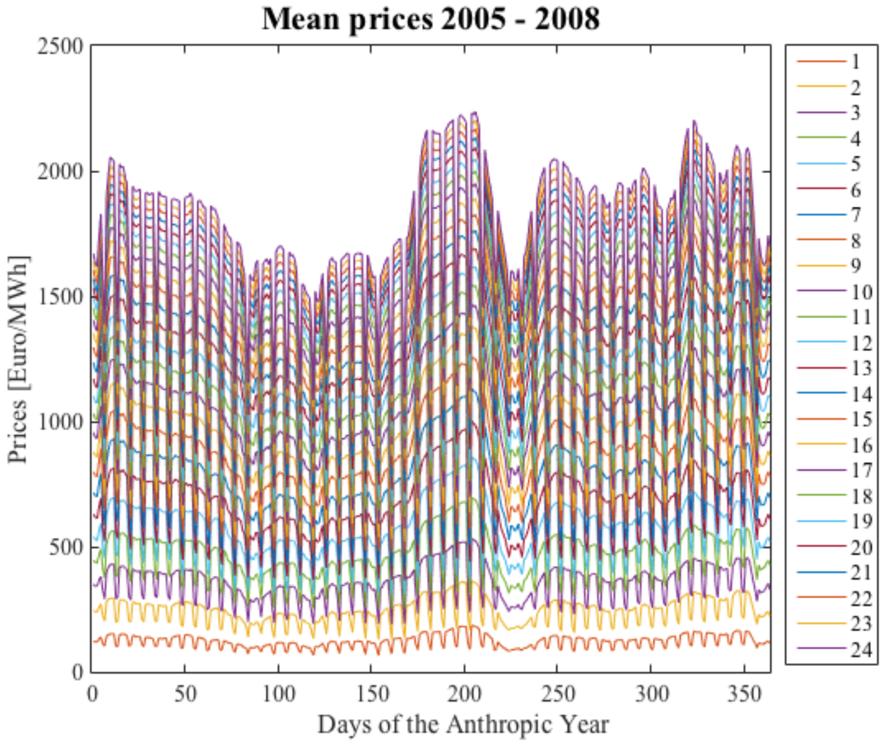

Figure 5-2: Mean energy prices on the period 2005 – 2008 cumulated from the lowest to the highest profitable hours

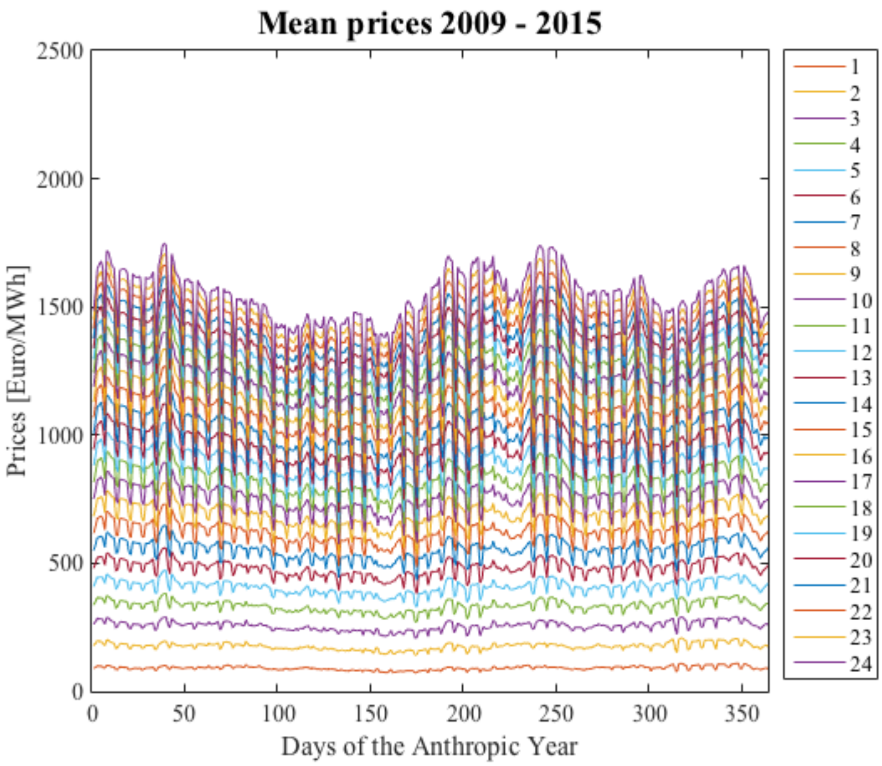

Figure 5-3: Mean energy prices on the period 2009 – 2015 cumulated from the lowest to the highest profitable hours

The comparison between Figure 5-2 and Figure 5-3 shows that the pre-renewable prices are more variable than the post-renewable prices: the difference between weekdays and weekend, as well as the variation from different periods of the year, is, in fact, more accentuated in the pre-renewable period. This is a well-know effect of the introduction of renewable energy sources in energy markets.

5.1 A2A and Enel systems

The system of A2A implemented in this thesis is composed by an equivalent reservoir, which merges together the reservoirs of San Giacomo and Cancano, and an equivalent power plant, created from the aggregation of the 4 power plants present in the system (Figure 5-4).
The maximum flow of the equivalent power plant is set to 41.06 m^3/s, which is the maximum flow of the Premadio power plant, the first plant downstream from the reservoirs and the energy coefficient is set to 3.365 KWh/m^3, equal to the sum of the energy coefficient of all the power plants.
The system of Enel implemented in this thesis is composed by an equivalent reservoir, which merged together the reservoirs of Alpe Gera and Campo Moro and an equivalent power plant, created from the aggregation of 2 power plants present in the system (Figure 5-4).
The maximum flow of the equivalent power plant is set to 23.55 m^3/s, which is the maximum flow of the first real power plant downstream of the reservoirs (Lanzada) and the energy coefficient is set to 3.66 KWh/m^3, equal to the sum of the energy coefficient of all the real power plants.

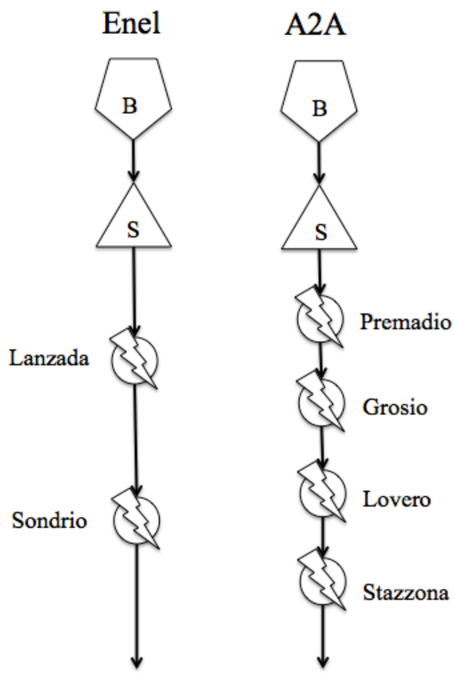

Figure 5-4: Enel and A2A conceptual hydropower systems

The minimum and maximum instantaneous release curves, shown in Figure 5-5 and Figure 5-6, describe the features of the equivalent reservoirs of A2A and Enel: the release from the reservoir is set, for any storage, with the following equation:

$$r_{t+1} = \min\left(\max(Q_{min}, u_t), Q_{max}\right)$$

where r_{t+1} $[m^3/s]$ is the release from the reservoir in the period [t, t+1), Q_{min} $[m^3/s]$ is the minimum release, u_t $[m^3/s]$ is the release decision taken at time t and Q_{max} $[m^3/s]$ is the maximum release.

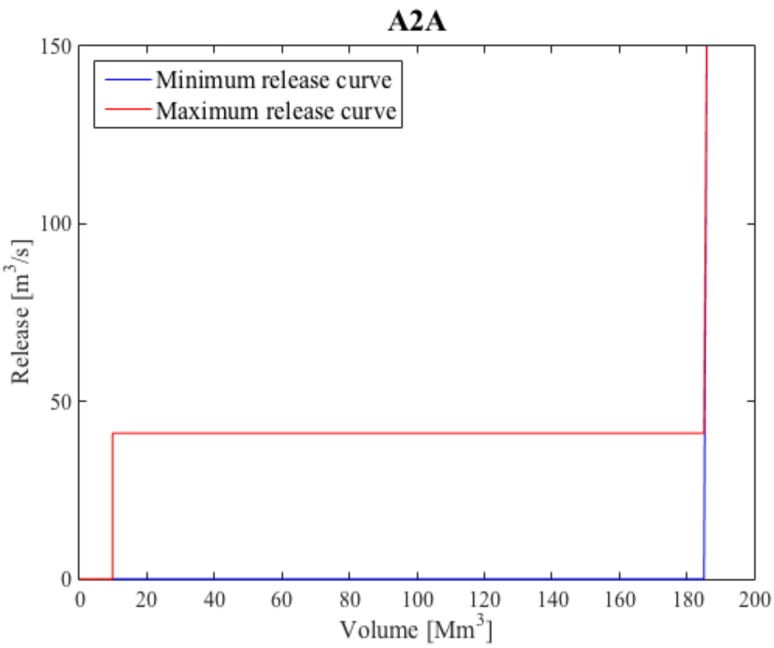

Figure 5-5: Minimum and maximum release curves for A2A equivalent reservoir

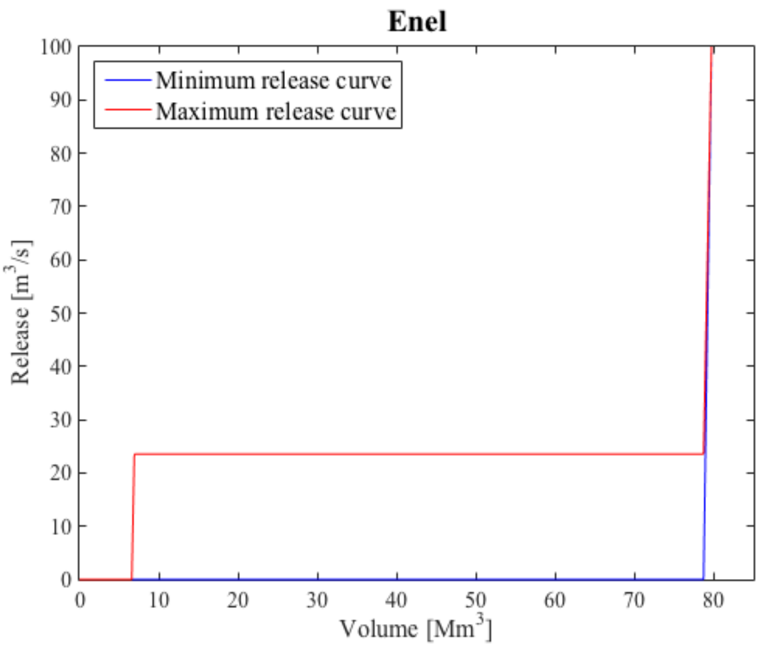

Figure 5-6: Minimum and maximum release curves for Enel equivalent reservoir

As explained in chapter 2.2, the implicit behavioural model we implement to describe the hydropower operators behaviour is based on SDP algorithm. SDP algorithm requires the probability distribution of the disturbance, which represents the inflow to the reservoir. This distribution, assumed to be lognormal, is computed starting from inflow time series on the period 1996-2014, through the definition of the cyclostationary (T=364, representing the anthropic time to be coherent with the price matrices) mean and the standard deviation.
Figure 5-7 and Figure 5-9 show the inflow time series and the average inflow per day of the anthropic year of A2A, while Figure 5-9 and Figure 5-10 show the inflow time series and the average inflow per day of the anthropic year of Enel.

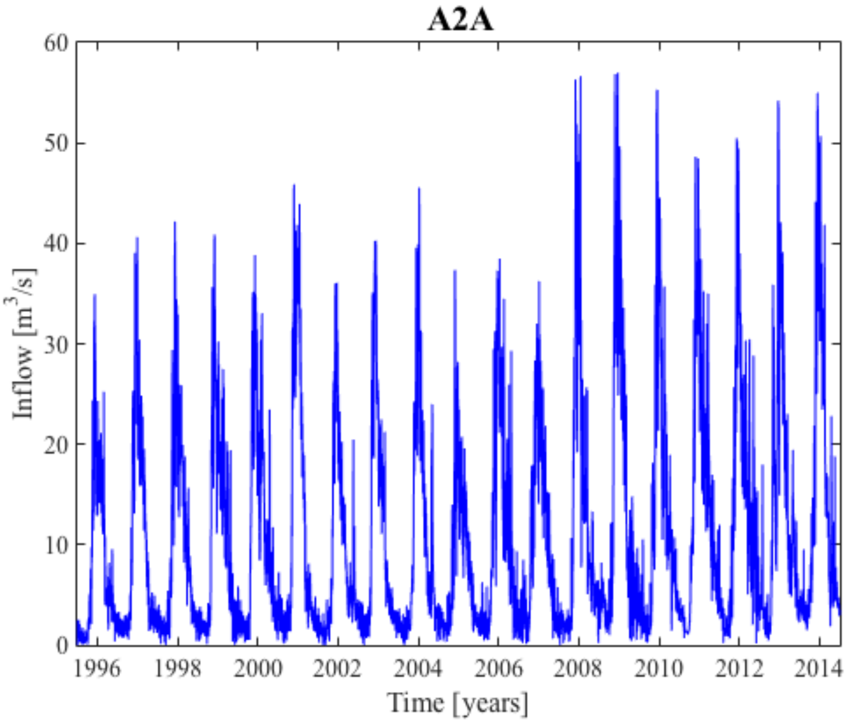

Figure 5-7: A2A inflow time series on the period 1996-2014

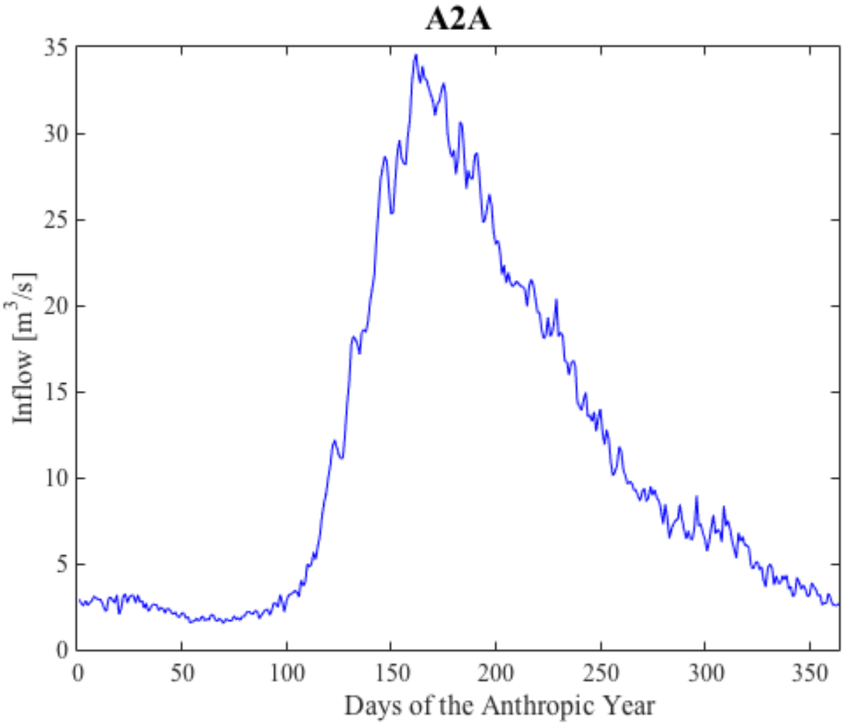

Figure 5-8: A2A average inflow per day of the anthropic year

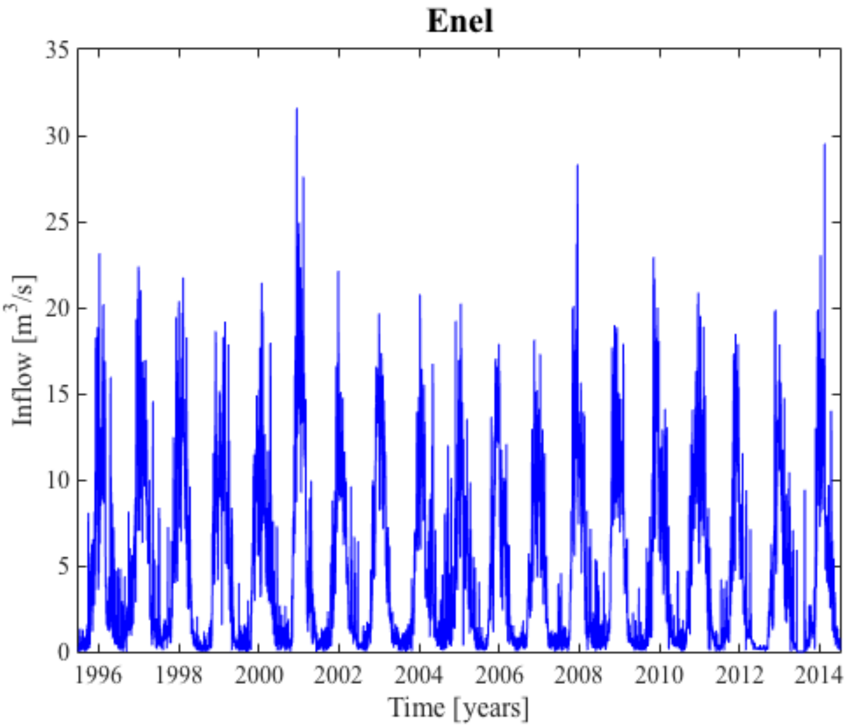

Figure 5-9: Enel inflow time series on the period 1996-2014

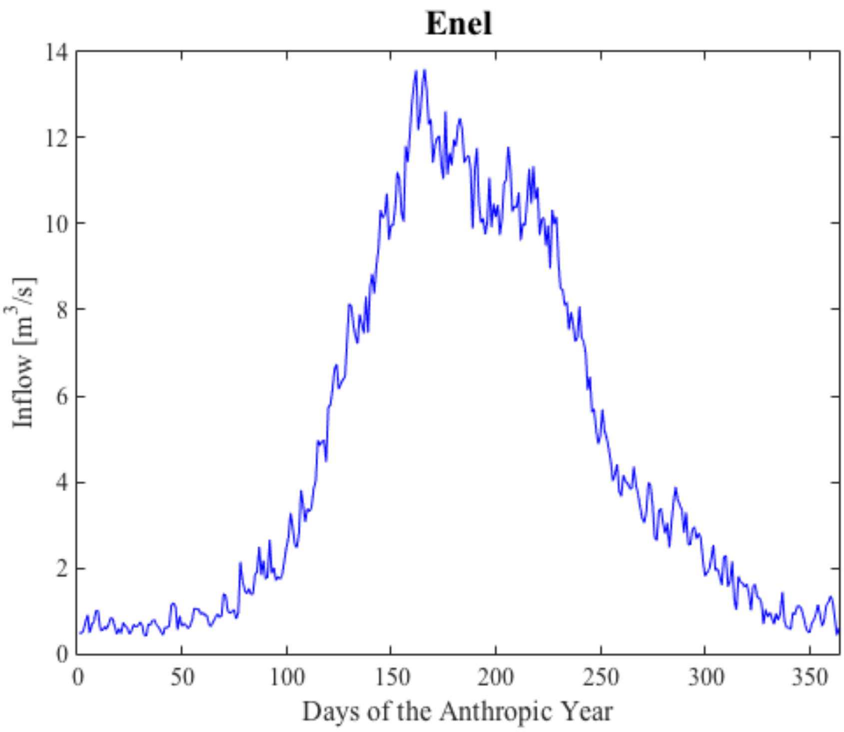

Figure 5-10: Enel average inflow per day of the anthropic year

Another operating hypothesis of SDP algorithm is that the system has to be an automaton: it is therefore necessary to implement a discretisation of all the variables of the model.
The inflow discretisation adopted for A2A is composed by 101 points that covers inflows from 0 m^3/s to 100 m^3/s with a regular step of 1 m^3/s.
The inflow discretisation adopted for Enel is composed by 51 points that covers inflows from 0 m^3/s to 50 m^3/s with a regular step of 1 m^3/s.
The discretisation adopted for the storage is not uniform: it is denser for low and high values, where we need to capture the abrupt change of the minimum and maximum release curves, and more loose for central values (Figure 5-5, Figure 5-6).

The discretisation of the release decision is uniform between the range [0, Q^T_{max}] and the step is defined as follow:

$$d = Q^T_{max}/24$$

where $d\ [m^3/s]$ is the step of discretisation and $Q^T_{max}\ [m^3/s]$ is the maximum flow of the turbine.
For instance, if the release decision is Q^T_{max} it means that the turbine produces energy for 24 hours in a day at the maximum flow.
The discretisation range of release decision for A2A reservoir is [0,41.06] with a step of 1.71 m3/s and the discretisation range of release decision for Enel reservoir is [0,23.55] with a step of 0.98 m3/s.

5.2 A2A and Enel results

The application of the SDP algorithm consists in an optimisation process, in which the algorithm generates an optimal policy.
In this thesis, the optimisation is performed, for each system, using the prices reported in Figure 5-2, for the pre-renewable scenario, and using the prices reported in Figure 5-3, for the post-renewable scenario. The systems are then simulated, using the optimal policies, in the pre-renewable period (2005-2008) and in the post-renewable period (2009-2014).

The comparisons between observed and simulated storage and release for the A2A reservoir are shown in Figure 5-11 and Figure 5-12 for the pre-renewable period and in Figure 5-13 and Figure 5-14 for the post-renewable period; the results for the Enel reservoir are shown in Figure 5-15 and Figure 5-16 for the pre-renewable period and in Figure 5-17 and Figure 5-18 for the post-renewable period.

The results show that the simulated release is always highly correlated to the price used in the optimization (Figure 5-2, Figure 5-3). In a model where the only objective is the revenue, the price represents, in fact, the main driver that influences the reservoir behaviour. As already explained, the price adopted in the optimisation and simulation phases is an average price, which cannot therefore capture its real annual variability. This is one of the reasons why the model is not always able to reproduce the historical data. Another issue is related to the real behaviour of the decision maker, which not always operates as a rational agent and, in some cases, is forced to operate in contrast to its interest because of constraints imposed from outside. For instance, observing Figure 5-17, it’s possible to note that in 2012 the Enel reservoir was almost completely emptied probably due to maintenance works: obviously the model is not able to capture this kind of situations. Finally, also the simplification related to the implementation of an equivalent reservoir may contribute to explain the differences between simulated and observed data, in particular for the Enel system: in this case in fact the equivalent reservoir is created merging together a big reservoir with a small one, which usually has more frequent storage fluctuations.

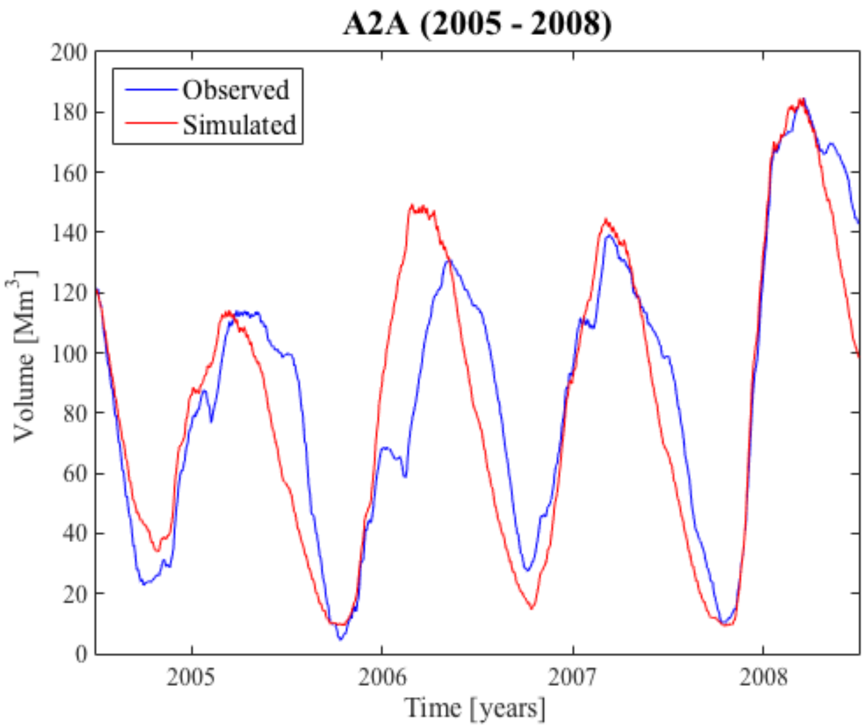

Figure 5-11: Comparison between observed and simulated storage in the pre-renewable period for the A2A reservoir

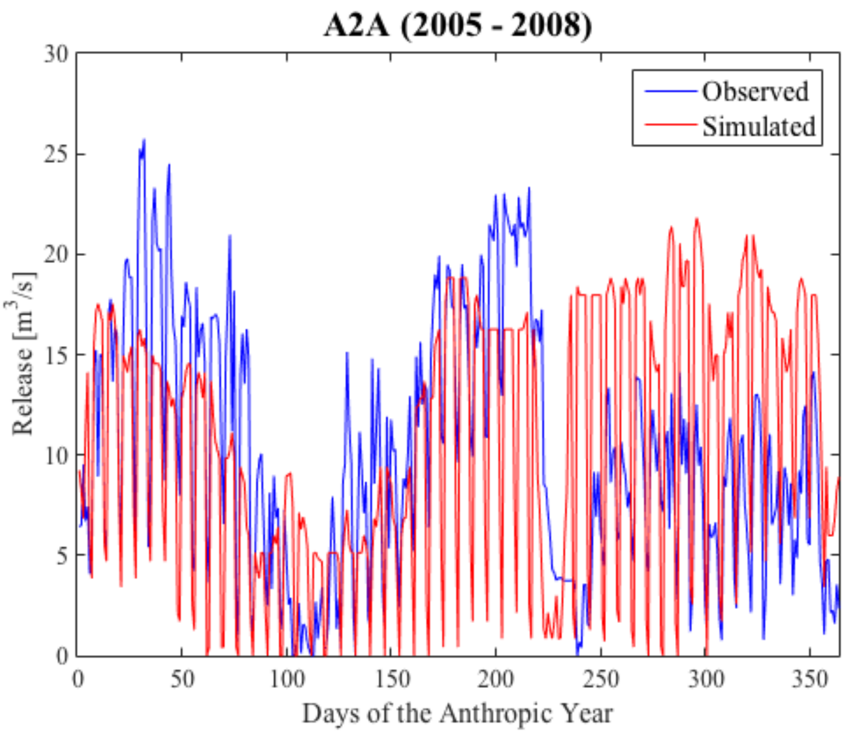

Figure 5-12: Comparison between observed and simulated average release per days of the anthropic year in the pre-renewable period for the A2A reservoir

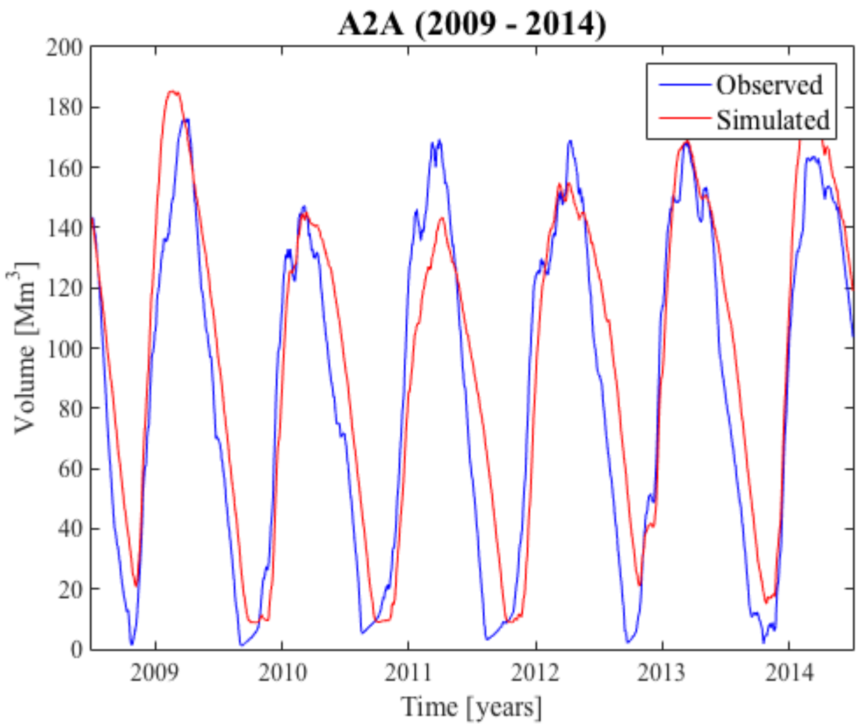

Figure 5-13: Comparison between observed and simulated storage in the post-renewable period for the A2A reservoir

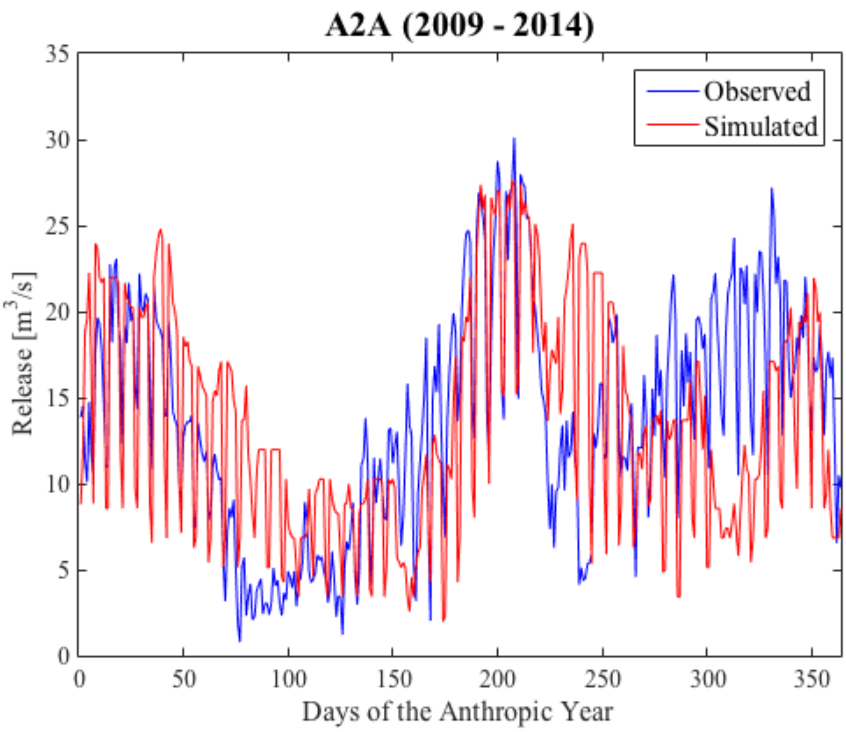

Figure 5-14: Comparison between observed and simulated average release per days of the anthropic year in the post-renewable period for the A2A reservoir

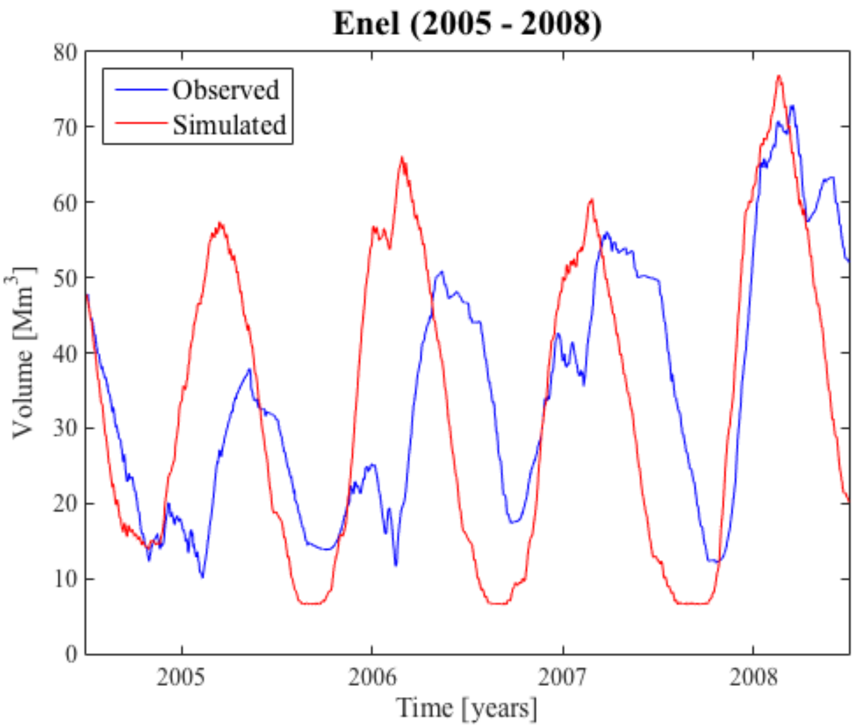

Figure 5-15: Comparison between observed and simulated storage in the pre-renewable period for the Enel reservoir

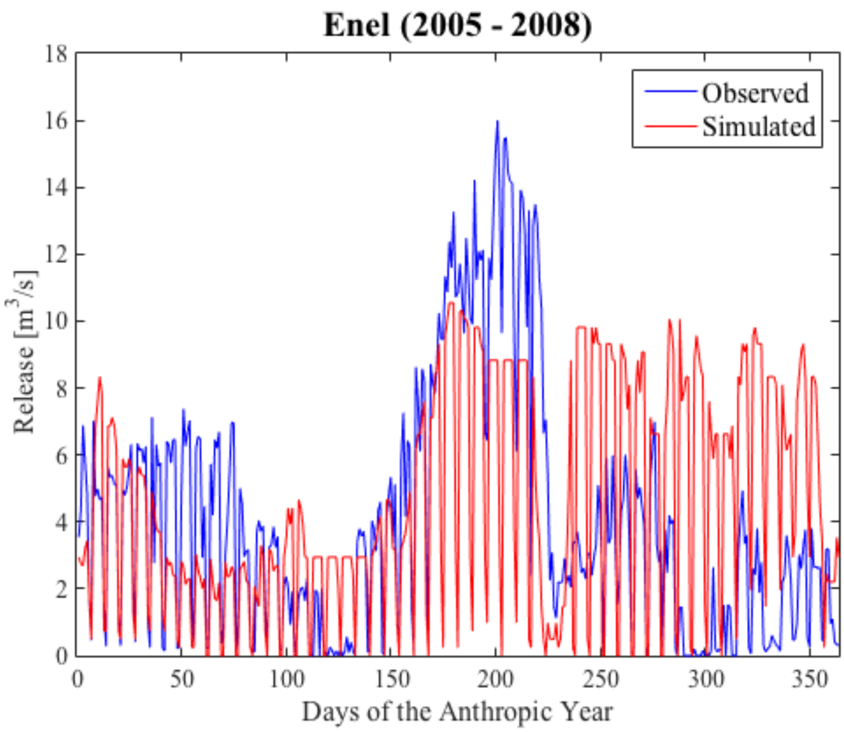

Figure 5-16: Comparison between observed and simulated average release per days of the anthropic year in the pre-renewable period for the Enel reservoir

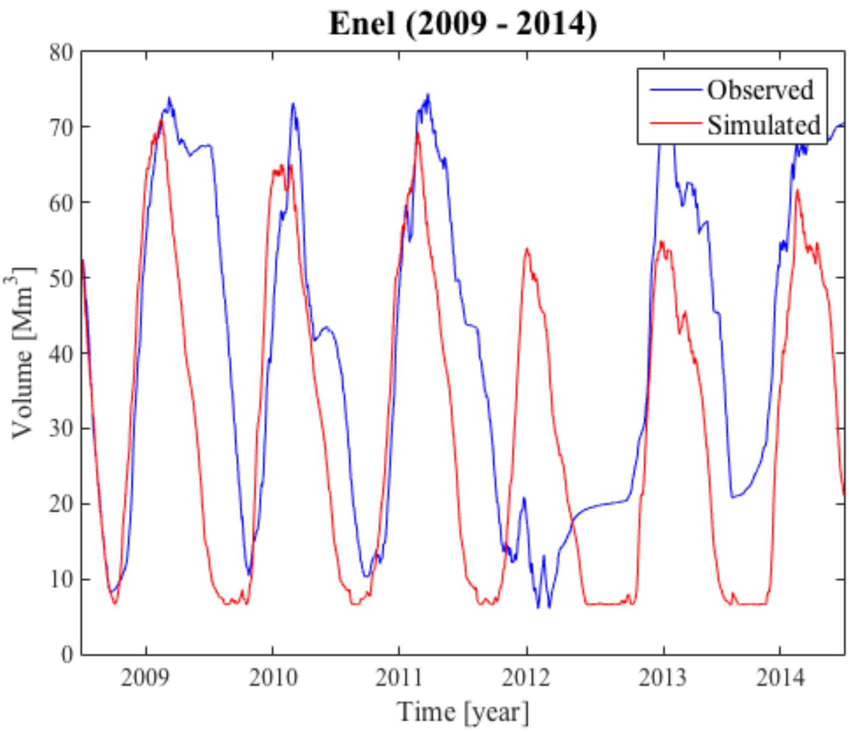

Figure 5-17: Comparison between observed and simulated storage in the post-renewable period for the A2A reservoir

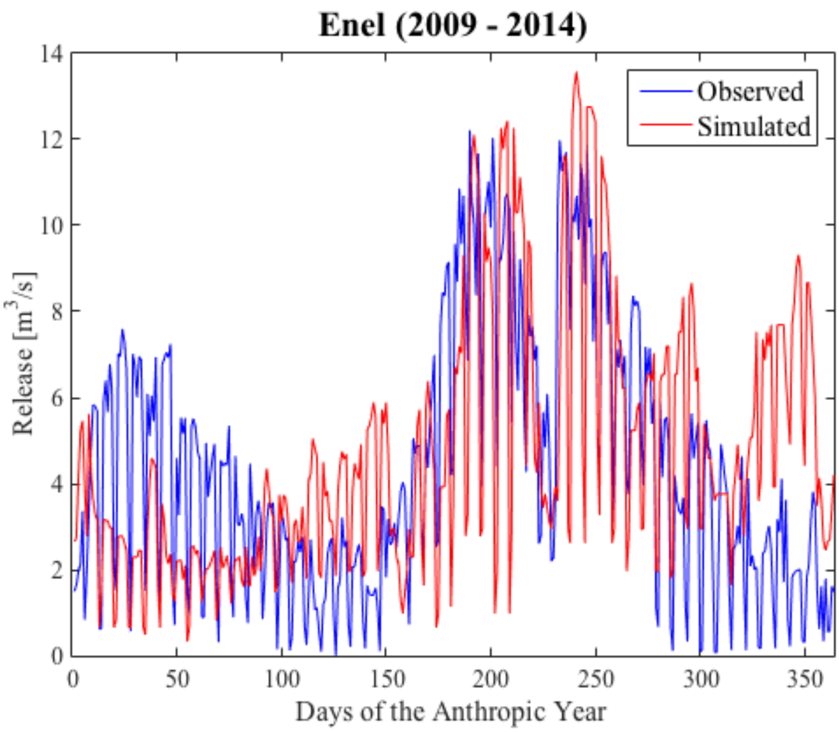

Figure 5-18: Comparison between observed and simulated average release per days of the anthropic year in the post-renewable period for the Enel reservoir

We also validate the model by computing the total energy production and the total revenue in the pre-renewable and post-renewable periods. The prices used for this kind of validation are the real prices observed in those periods in order to obtain results closer to the reality. The production and the revenue, normalized on the historical performances[1], are shown in Figure 5-19 for A2A and in Figure 5-20 for Enel.

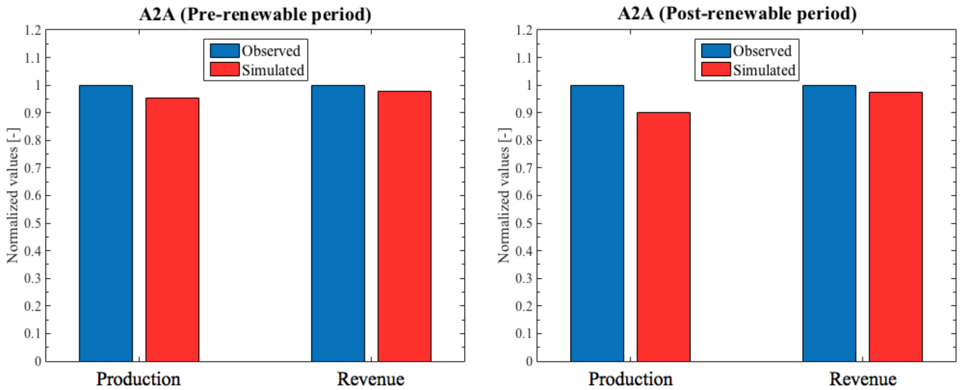

Figure 5-19: Observed and simulated production and revenue for the A2A reservoir

The A2A simulated production and revenue are underestimated with respect to the observation: the differences in the production are about 5% in the pre-renewable period and about 10% in the post-renewable period; the differences in the revenue are about 2% in the pre-renewable period and about 3% in the post-renewable period.

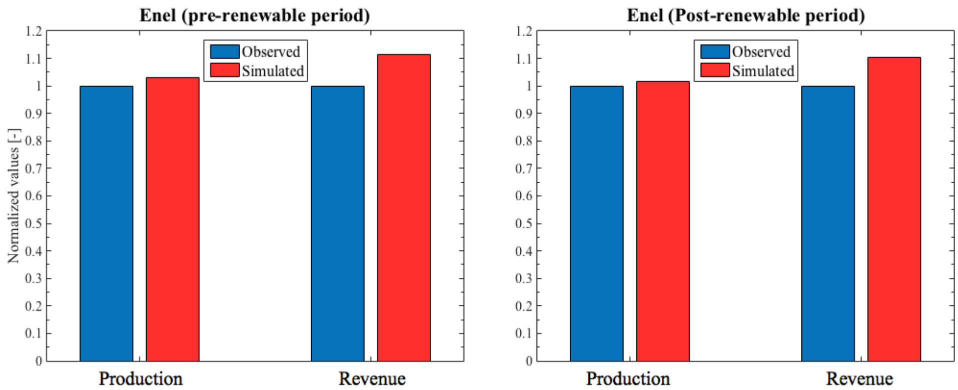

Figure 5-20: Observed and simulated production and revenue for the Enel reservoir

The Enel simulated production and revenue are overestimated with respect to the observation: the differences in the production are about 3% in the pre-renewable period and about 1.6% in the post-renewable period; the differences in the revenue are about 11% in the pre-renewable period and about 10.5% in the post-renewable period.
The overestimation in the post-renewable period is probably affected by the closure of the reservoir for maintenance activities occurring in 2012 (Figure 5-17), instead, the overestimation in the pre-renewable period is probably due to external constraints (e.g., forced release due to

[1] The historical performances are determined calculating the objective function implemented in the model using the historical release.

environmental/normative constraints) that have affected the operator behaviour (Figure 5-15).

5.3 Effect of different price scenarios on reservoirs' management

One of the objectives of this thesis is to assess how CHNS react to changes in socio-economic drivers. As explained in chapter 2, changes in socio-economic drivers don't affect the hydrology upstream of the reservoirs, but may affect the hydrology downstream of the reservoir through changes in the operators' behaviour.
In this section, we analyse the behaviour of hydropower systems in response to changes in socio economic drivers, represented in our case by the energy prices. We perform, for each system, two different simulations over the period 1996-2014: one with the policy optimized with the pre-renewable prices and the other with the policy optimized with the post-renewable prices.

As already explained, the price in the post-renewable period has a smaller variability between weekdays and weekends than the price in the pre-renewable period. Since the release is highly dependent upon the price, we can notice that, for both the systems, the release has a less weekdays-weekends variability in the post-renewable period than in the pre-renewable period.
The two systems react instead in different ways to changes in the variability of the price between different seasons of the year.
When this variability is high (e.g. pre-renewable period), the behaviour of the reservoir follows the pattern of the price, because it defines univocally when releasing is more profitable (Figure 5-21, Figure 5-24).
On the contrary, when the variability is low (e.g. post-renewable period), there are some periods of the year in which releasing produces almost the same revenue. In these situations the disturbance, (inflow) together with the price drive the reservoir dynamics.

As shown in Figure 5-25, Enel concentrates the release decision in the period between 200 and 250 (days of the anthropic year), when the prices are the highest in the year (Figure 5-3) and the volume of the reservoir oscillates around its maximum capacity: an high inflow in that period (Figure 5-26) could, in fact, activate the spillways, with the consequent lost of turbinable flow. A2A, which in the same period receives a lower inflow (Figure 5-23), prefers instead to distribute the release decision along all the high price periods of the year (Figure 5-22).

The hydrological effects of different reservoirs management in response to changes in the socio-economic drivers are described in chapter 7.

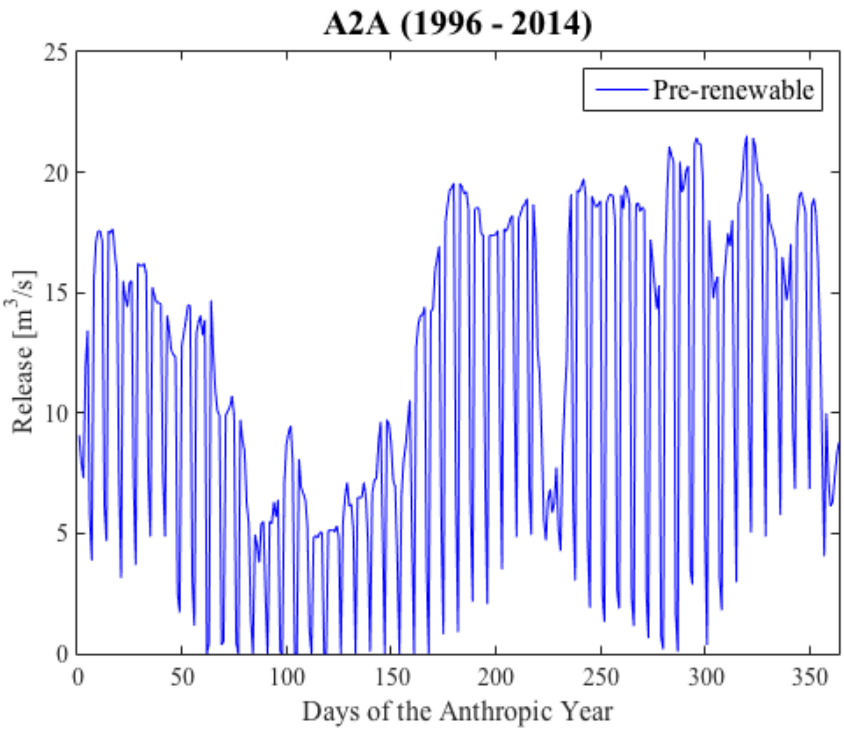

Figure 5-21: Simulated average release per day of the anthropic year for A2A reservoir in the pre-renewable scenario

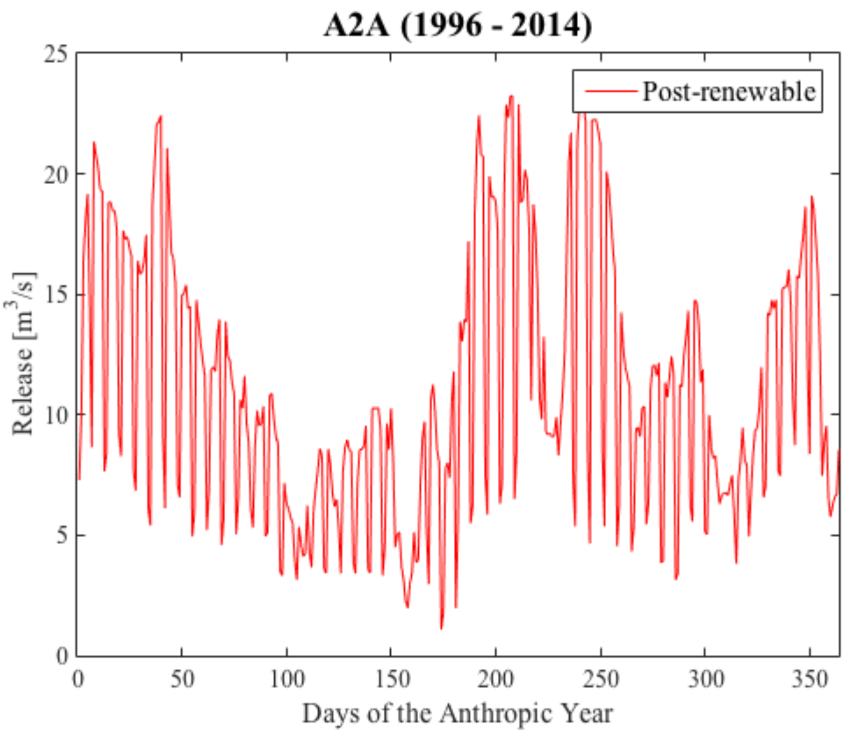

Figure 5-22: Simulated average release per day of the anthropic year for A2A reservoir in the post-renewable scenario

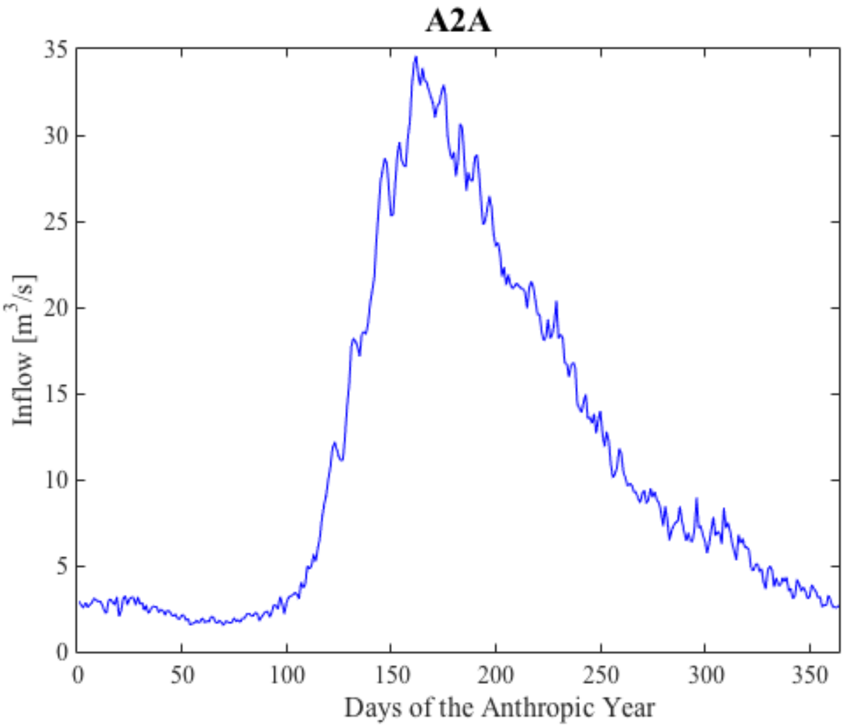

Figure 5-23: Average inflow per day of the anthropic year of the A2A reservoir

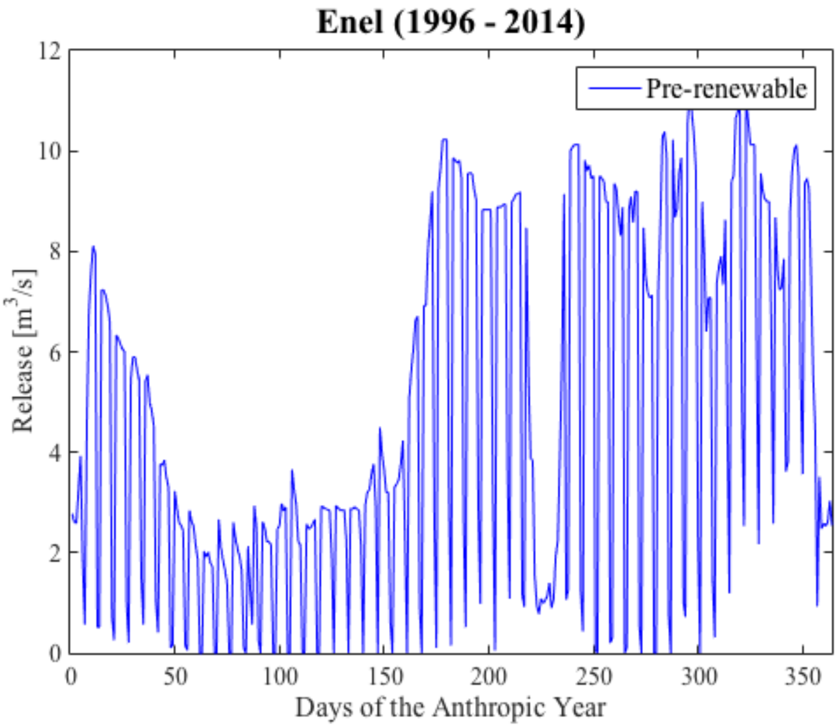

Figure 5-24: Simulated average release per day of the anthropic year for Enel reservoir in the pre-renewable scenario

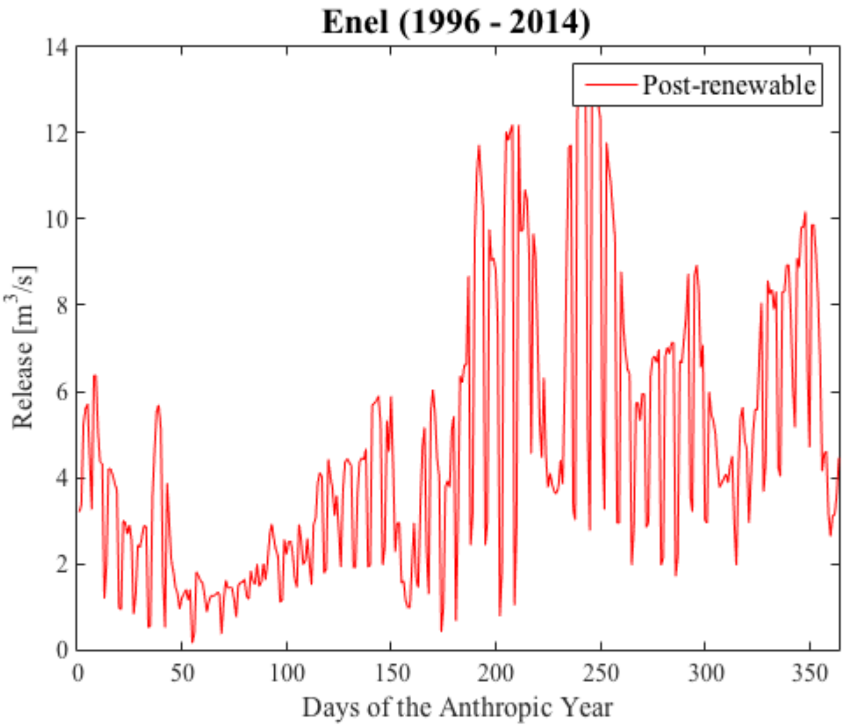

Figure 5-25: Simulated average release per day of the anthropic year for Enel reservoir in the post-renewable scenario

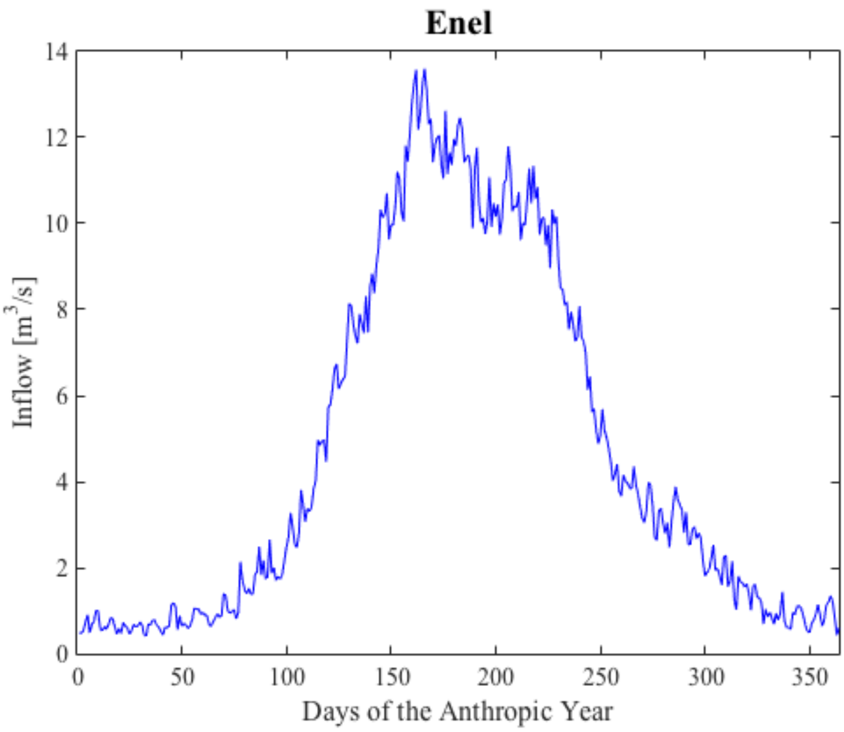

Figure 5-26: Average inflow per day of the anthropic year of the Enel reservoir

6 Topkapi-ETH: behavioural model integration

Topkapi-ETH "reservoirs module" allows simulating the reservoirs dynamic through a mass balance volume. Since Topkapi-ETH works on a grid cell basis (see chapter 2.1), the reservoirs can be represented by multiple cells. The volume of the reservoir is computed considering all the water entering the reservoir cells through surface, soil, channel, or precipitation and the water losses through evaporation and infiltration/exfiltration. For the sake of simplicity, we refer to the reservoir as a unique object in this chapter, without explicitly referring to all the cells representing the reservoir.
The reservoirs structural features are defined through external input files and specified in the model configuration file.
The external input files defining the reservoirs structural features are:

- *h-V table* (Figure 6-1) defining the relationship between level and volume for each reservoir
- *h-Q_{max} table* (Figure 6-1) defining relationship between level and the maximum allowable outflow for each reservoir: when the level is under the dead level, the maximum allowable outflow is set to zero; when the level is between the dead level and the maximum level, the maximum allowable outflow is set to the maximum flow of the turbine; when the level is over the maximum level, the maximum allowable outflow, which in this case is equal to the minimum allowable outflow, is set to the maximum flow of the turbine plus the flow of the spillways (Figure 6-2).

Reservoirs_HV.dat

ID	h	V
1.0000000e+00	1.9249467e+03	0.0000000e+00
1.0000000e+00	1.9253672e+03	7.8850000e+05
1.0000000e+00	1.9257877e+03	1.5770000e+06
1.0000000e+00	1.9262083e+03	2.3655000e+06
1.0000000e+00	1.9266288e+03	3.1540000e+06
1.0000000e+00	1.9270493e+03	3.9425000e+06
1.0000000e+00	1.9274699e+03	4.7310000e+06
1.0000000e+00	1.9278904e+03	5.5195000e+06
1.0000000e+00	1.9640563e+03	7.3330500e+07
1.0000000e+00	1.9653179e+03	7.5696000e+07
1.0000000e+00	1.9657384e+03	7.6484500e+07
1.0000000e+00	1.9661589e+03	7.7273000e+07
1.0000000e+00	1.9665795e+03	7.8061500e+07
1.0000000e+00	1.9670000e+03	7.8850000e+07
1.0000000e+00	1.9674000e+03	7.9688000e+07
1.0000000e+00	1.9680000e+03	8.0688000e+07
1.0000000e+00	5.0511067e+03	5.5770000e+08
2.0000000e+00	1.8820370e+03	0.0000000e+00
2.0000000e+00	1.8822267e+03	3.2000000e+05
2.0000000e+00	1.8824163e+03	6.4000000e+05
2.0000000e+00	1.8826059e+03	9.6000000e+05
2.0000000e+00	1.8827956e+03	1.2800000e+06
2.0000000e+00	1.8829852e+03	1.6000000e+06
2.0000000e+00	1.8831748e+03	1.9200000e+06
2.0000000e+00	1.8833644e+03	2.2400000e+06
2.0000000e+00	1.8835541e+03	2.5600000e+06
2.0000000e+00	1.8837437e+03	2.8800000e+06
2.0000000e+00	1.8839333e+03	3.2000000e+06
2.0000000e+00	1.8841230e+03	3.5200000e+06
2.0000000e+00	1.8939837e+03	2.0160000e+07
2.0000000e+00	1.8987244e+03	2.8160000e+07
2.0000000e+00	1.9006207e+03	3.1360000e+07
2.0000000e+00	1.9008104e+03	3.1680000e+07
2.0000000e+00	1.9010000e+03	3.2000000e+07
2.0000000e+00	5.9389259e+03	20.4000000e+07

Reservoirs_HQ.dat

ID	h	Q_max
1.0000E+00	1.9249E+03	0.0000E+00
1.0000E+00	1.9254E+03	0.0000E+00
1.0000E+00	1.9258E+03	0.0000E+00
1.0000E+00	1.9262E+03	0.0000E+00
1.0000E+00	1.9266E+03	0.0000E+00
1.0000E+00	1.9270E+03	0.0000E+00
1.0000E+00	1.9275E+03	0.0000E+00
1.0000E+00	1.9279E+03	0.0000E+00
1.0000E+00	1.9283E+03	0.0000E+00
1.0000E+00	1.9285E+03	0.0000E+00
1.0000E+00	1.9286E+03	2.3550E+01
1.0000E+00	1.9657E+03	2.3550E+01
1.0000E+00	1.9662E+03	2.3550E+01
1.0000E+00	1.9666E+03	2.3550E+01
1.0000E+00	1.9670E+03	2.3550E+01
1.0000E+00	1.9674E+03	1.0000E+02
1.0000E+00	1.9680E+03	1.5000E+02
1.0000E+00	2.0150E+03	2.0000E+02
2.0000E+00	1.8820E+03	0.0000E+00
2.0000E+00	1.8822E+03	7.5000E+00
2.0000E+00	1.8949E+03	7.5000E+00
2.0000E+00	1.8972E+03	7.5000E+00
2.0000E+00	1.8993E+03	7.5000E+00
2.0000E+00	1.8995E+03	7.5000E+00
2.0000E+00	1.8997E+03	7.5000E+00
2.0000E+00	1.8999E+03	7.5000E+00
2.0000E+00	1.9001E+03	7.5000E+00
2.0000E+00	1.9002E+03	7.5000E+00
2.0000E+00	1.9006E+03	7.5000E+00
2.0000E+00	1.9008E+03	7.5000E+00
2.0000E+00	1.9010E+03	7.5000E+00
2.0000E+00	1.9389E+03	7.5000E+00

Figure 6-1: h-V table *and* h-Q_{max} table *examples in case of 2 reservoirs*

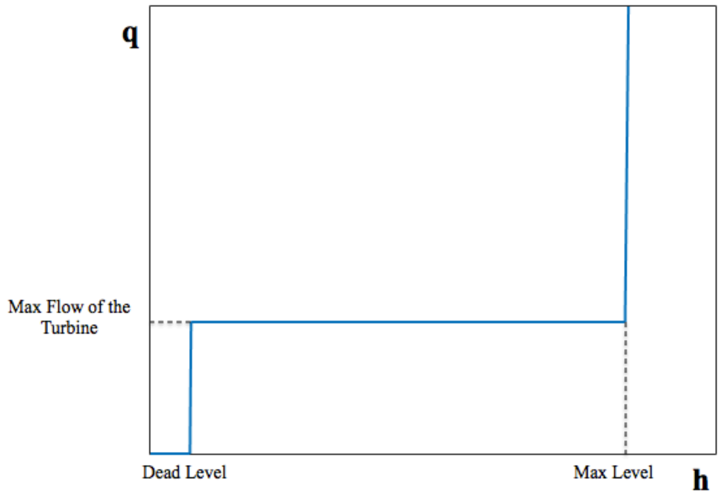

Figure 6-2: h-Q_{max} table

The model configuration file should contain the following information, for each reservoir implemented:

- *ID*: reservoir identification number
- *Outlet Code*: identification of the grid cell representing the reservoir outlet (e.g., the cell where the reservoir outflows is returned into the river network)
- *Initial Volume*: reservoir volume at the beginning of the simulation
- *Res Active*: boolean variable stating if the reservoir is active or not (if not, the reservoir cells are treated as soil or river cells)
- *Simulation Mode*: identification of the reservoir simulation mode

As previously mentioned, we compare two different simulation modes: the first in-built simulation mode aims at tracking a target level; the second simulation mode was, instead, implemented in this thesis[2] and aims at representing the reservoirs operators behaviour following an operating policy obtained as the solution of a control problem (see chapter 5). The following chapters 6.1 and 6.2 describe in details the two simulation modes.

6.1 Reservoirs simulation mode based on "target level"

This simulation mode requires the definition of a "target level" in the form of a time series of levels for each *simulation time step*.
The *simulation time step* is usually daily or hourly, but in both cases the reservoirs module works on a minute based *integration time step*: the module is therefore executed 1440 times per *simulation time step*, if a daily *simulation time step* is adopted, and 60 times per *simulation time step*, if a

[2] This simulation mode has been implemented using the Fortran language to be fully compliant with Topkapi-ETH source code. Furthermore, we have made the effort to remain consistent with the program setting and the architectural design.

hourly *simulation time step* is adopted.
The flowchart in Figure 6-3 shows the functioning of this simulation mode. The maximum volume of the reservoir is read from the *h-V table* at the beginning of the simulation and, at each *integration time step,* the current reservoir volume is compared to the maximum volume: if it's higher the execution of the program end with an error, otherwise, the execution continues, setting the value to zero if it's negative.
The current volume is then converted in level through the *h-V table* and the level is compared with the target level of the current *simulation time step*. If the level is higher than the target level, the release from the reservoir is set to the maximum feasible outflow through the h-Q_{max} *table*, otherwise the release is set to zero.
Finally the mass balance equation computes the volume of the next *integration time step*: at the end of this cycle, the release of the current *simulation time step* is set as the average release of all the integration time steps and the volume of the next *simulation time step* is updated.
We have to note that the target level is defined according to the *simulation time step* and therefore it doesn't change inside the *integration time step* cycle.

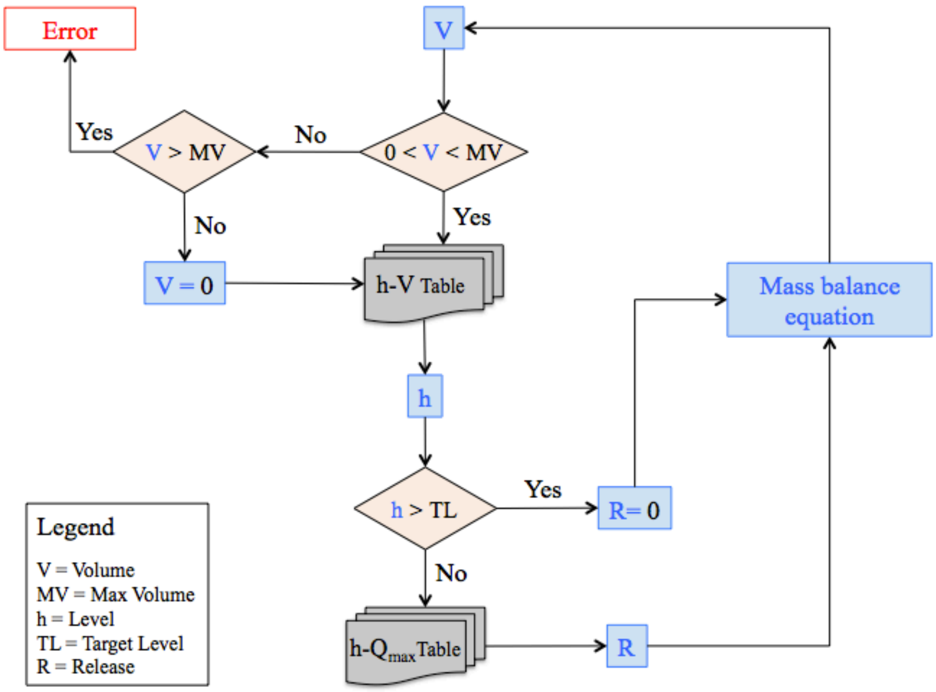

Figure 6-3: Flow chart of "target level" based simulation

6.2 Reservoirs simulation mode based on "optimized policy"

This simulation mode simulates the reservoir dynamic by means of an optimized policy, independently obtained as the solution of a control

problem (see chapter 5). The optimized policy we generate by an SDP algorithm is a function that defines, for each day of the anthropic year and for each reservoir storage discretisation, the optimal release decision. This function is therefore cyclostationary of period T=364.
Because of implementation problems, we cannot manage the anthropic time in Topkapi-ETH and therefore we need to represent the optimized policy as a table that explicitly defines, for each simulation time step and for each reservoir storage discretisation, the optimal release decision. Furthermore, the reservoir storage discretisation used to solve the control problem has to be provided separately by the definition of a proper input.
This simulation mode requires the following inputs/information for each reservoir:

- *Policy table* defining, for each reservoir, the optimal release for each *simulation time step* as a function of the storage (according to the storage discretization)
- *Storage discretisation* defining, for each reservoir, the storage discretisation adopted to solve the control problem through SDP
- *Dead level* defining the level under which the release is constrained by the physical reservoir features
- *Maximum level* defining the level above which the release is constrained by the spillways' rating curve

In addition to the simulation and integration time steps, we need to introduce the *decision time step* in this simulation mode, in order to accurately simulate the real decision processes. The decision time step defines the moment when the release decision is taken. In the real decision processes, the release decision is usually taken at fixed intervals (e.g., once a day) with the exception of particular situations in which the decision is taken more frequently to manage exceptional events (e.g., flood events). However in normal operational conditions, the decision time step must be short enough to allow a timely adjustment of the decision as the state of the system varies but it should not be so short as to create social, economic or organizational difficulties for the reservoirs operators [Soncini-Sessa et al., 2007].

The *simulation time step* is usually daily or hourly but the reservoir module works on a minute based *integration time step*, which is usually too short for the decision maker: in fact, except in special cases (e.g., critical issues balancing the electrical grid), taking decision every minute doesn't make sense. If we adopt an hourly *simulation time step*, we can choose a daily or a hourly *decision time step*, instead, if we adopt a daily *simulation time step*, as in the case study considered in this thesis, the *decision time step* is daily and the release decision is taken, by default, at the beginning of the day.

Figure 6-4 describes the simulation algorithm. At the beginning of each *simulation time step*, e.g. at each first *integration time step*, the release decision is retrieved from the *Policy table* using the current *simulation time*

step and the current volume. The volume is then converted in level through the *h-V table* and the level is compared with the *Dead level* and *Maximum level*: if the current level fall between the *Dead level* and the *Maximum level*, the release from the reservoir is set equal to the decision, otherwise, the release is retrieved from the *h-Q_{max} table*.
Finally the mass balance equation computes the volume of the next *integration time step*: at the end of this cycle, the release of the current *simulation time step* is set as the average release of all the integration time steps and the volume of the next *simulation time step* is updated.

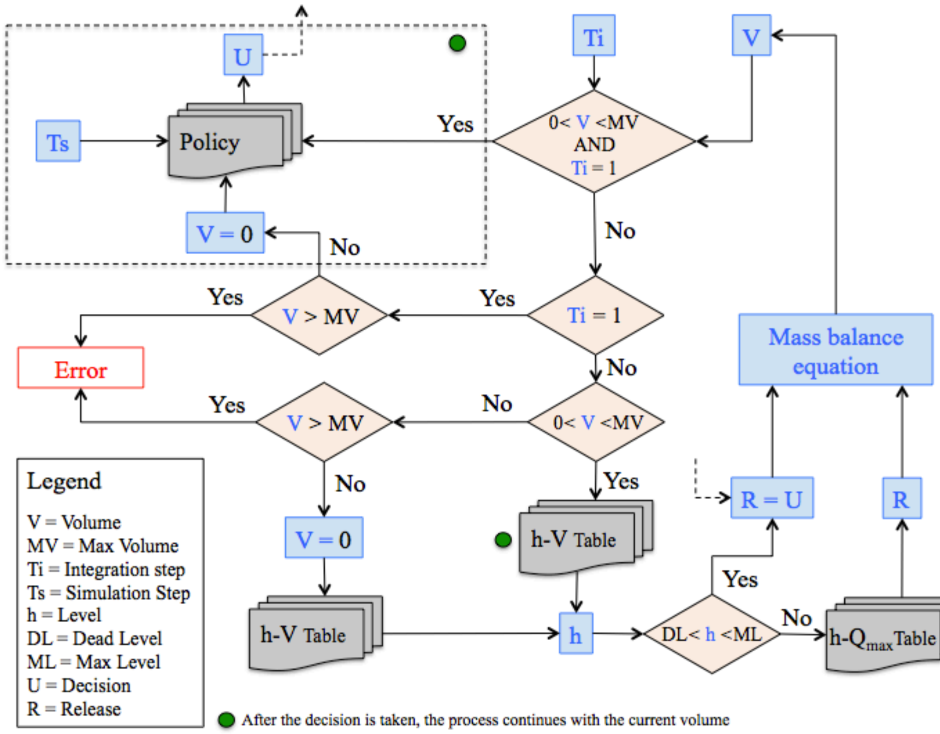

Figure 6-4: Flow chart of the "optimized policy" based simulation

A further development of Topkapi-ETH, concerning this simulation mode, could be the internal management of the anthropic time: in this way, it is no longer necessary to define the policy table for each simulation time step but only for T time step, where T is the period of the cyclostationary policy.

7 Simulation experiments

The main objective of this thesis is to compare the differences that may arise from the inclusion of simple and advanced reservoirs operating rules in CHNS models in order to assess the relationship and the feedbacks that exist between natural and human components.
In this chapter, we implement some numerical experiments to evaluate the effects of simple and advanced operating rules on the reservoirs dynamics, on the hydropower performance and on the hydrological regime (Figure 7-1), (Table 7-1). The simple operating rules are based on a target level, as described in chapter 6.1, instead the advanced operating rules are based on an optimized policy, as described in chapter 6.2.
We simulate Topkapi-ETH on the period 2006-2013, setting first the reservoirs simulation mode based on target level and then the simulation mode based on an optimized policy. The comparison between different simulation modes on the reservoirs dynamics is assessed in terms of reservoirs storage and release (chapter 7.1) and in terms hydropower performances (chapter 7.2).
The effect of different simulation modes on the hydrological regime is instead evaluated through the comparison of the flow in different sections of the basin (chapter 7.3).
For the sake of simplicity, we show the results focusing on the A2A reservoir, which is the main reservoir of the catchment.

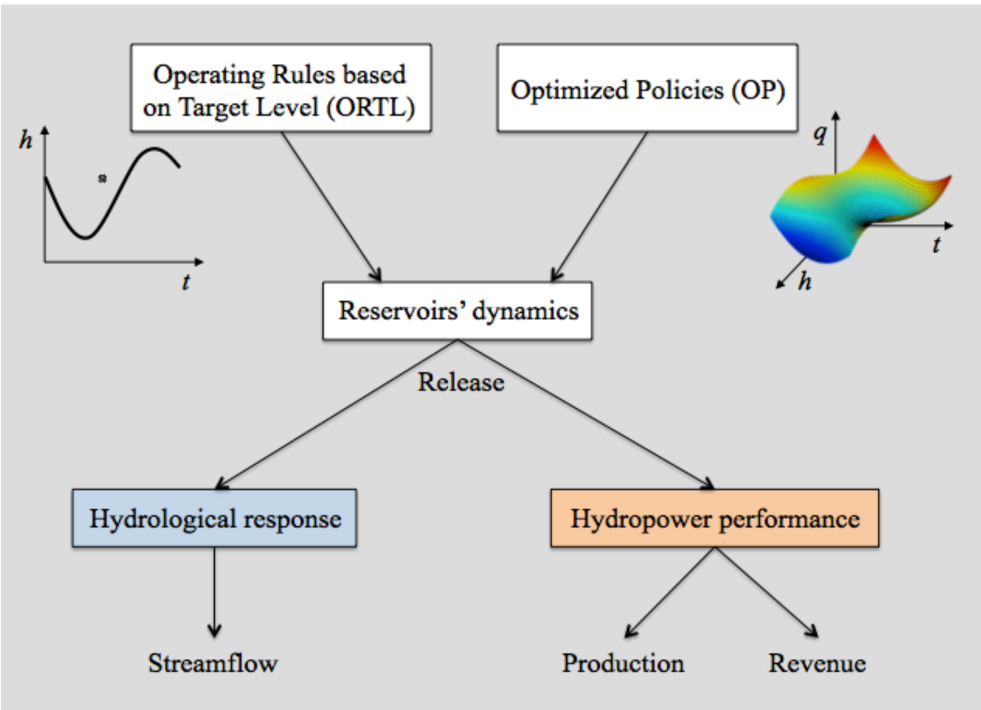

Figure 7-1: Scheme of the simulation experiments

Simulation Experiments					
	Simulation 1	**Simulation 2**	**Simulation 3**	**Simulation 4**	**Comparison Results**
Reservoir dynamics	ORTL (Natural time)	ORTL (Anthropic time)	OP (Pre-renewable)	-	Storage/Release
Hydropower performance	ORTL (Natural time)	ORTL (Anthropic time)	OP (Pre-renewable)	-	Production/Revenue
Hydrological response	ORTL (Natural time)	-	OP (Pre-renewable)	OP (Post-renewable)	Streamflow in different sections of the basin

ORTL: Operating Rule based on Target Level
OP: Optimized Policy

Table 7-1: Simulation experiments

7.1 Different reservoirs dynamics in response to simple and complex operating rules

The comparison between simple and complex operating rules is evaluated through different simulations in the period 2006-2013.
The optimal policy adopted for the comparison is the policy calculated for the pre-renewable scenario, as described in chapter 5.
The target level, which represents the reference trajectory that defines the reservoirs operational behaviour during a normal hydrological year, is instead calculated, from the historical observations of storage on the period 2006-2013, computing a cyclostationary mean of period T=365 based on the natural time. According to the natural time definition, each day is identified by an ordinal number (1-365/366) that labels it with respect to the first day of the year (day 1) [Soncini-Sessa et al., 2007].

For consistency with the choice of the optimal policy, it would be appropriate to calculate the target level in the pre-renewable period, but in so doing, only few years would be available (2006-2008).

The comparison between the two simulation modes in terms of storage is shown in Figure 7-2. In the simulation based on target level, the storage always follows the reference trajectory, according to the operating rule described in chapter 6.1 (see black line in Figure 7-2). In this way, the model cannot capture the inter-annual variability of the storage, which instead occurred in the historical observation. This variability is mainly caused by variability in the inflow to the reservoir, both in terms of volume and timing, which may affect the behaviour of the operators.
The storage variability is represented by the annual variance of the observed storage: the more this variance is high, the more the target level is not able to describe the historical pattern of the storage and, therefore, the performance of the model in reproducing the reservoir dynamic decreases.
So, when there is a high inter-annual variability, this simulation mode is not suitable to correctly represent the reservoirs behaviour and it may be more appropriate to simulate the reservoirs dynamics with more complex operating rules, which are able, besides the storage, to explicitly account for the inflow stochasticity. The simulation based on an optimized policy, which is computed considering also the inflow distribution, is in fact able to capture the inter-annual variability of the storage (see blue line in Figure 7-2).

Another difference between the two simulation modes can be observed comparing the release from the reservoir (Figure 7-3).
The high variability of the release reproduced by the simulation based on an optimized policy is due to the high weekdays-weekends variability of the energy price, which decrease significantly during the weekends due to the decrease of the energy demand: the optimal release is, in fact, higher during weekdays, when selling the energy is more profitable, and lower in the weekends. The simulation based on target level instead does not capture the different hydropower behaviour during weekdays and weekends. This is due to the use of the natural time in the definition of the target level: in fact the natural time doesn't allow distinguishing between weekdays from weekends.

When the focus is on the hydrology, this approach still let obtain good results in capturing the seasonal volume shift due to the reservoirs behaviour, but when the focus is also on hydropower, describing the weekdays-weekend variability become essential.

Therefore we perform a further simulation experiment calculating the target level, computing a cyclostationary mean of period T=364 based on the anthropic time. The anthropic time aligns all the first Monday of the year and therefore allows keeping distinct weekdays from weekends.

The results show that, the main seasonal dynamic of the storage is almost the same in the simulation performed using a target level based on the anthropic time (red line in Figure 7-4) and in the simulation performed using a target level based on the natural time (black line in Figure 7-4), but the simulation performed using a target level based on the anthropic time can capture the weekdays-weekends variability of the release (Figure 7-5).

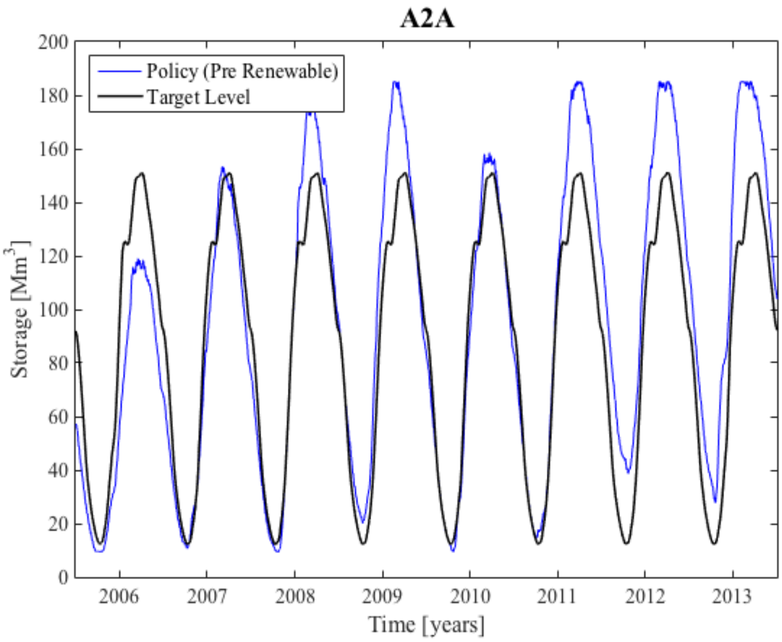

Figure 7-2: Storage obtained from different simulation modes (policy, target level based on natural time) for the A2A reservoir

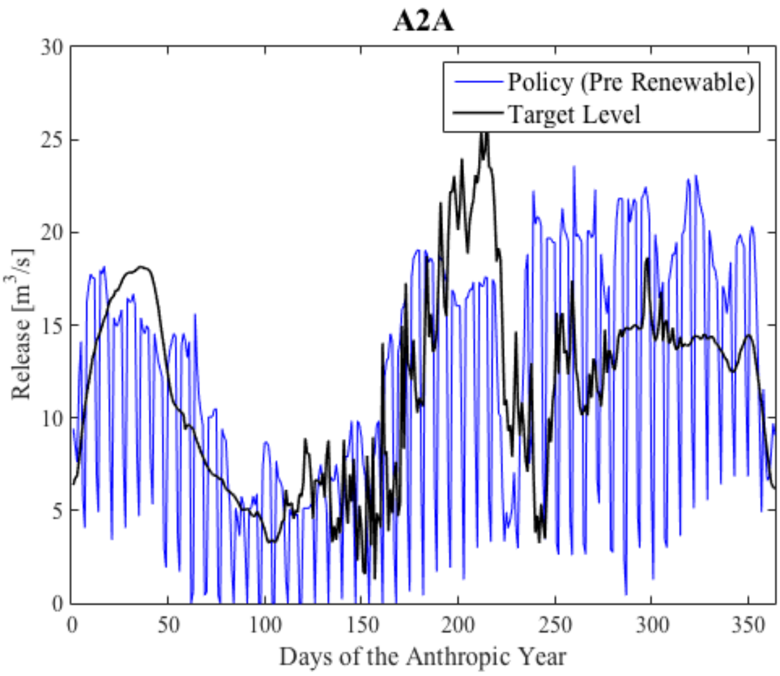

Figure 7-3: Average release per day of the anthropic year obtained by different simulation modes (policy, target level based on natural time) for the A2A reservoir

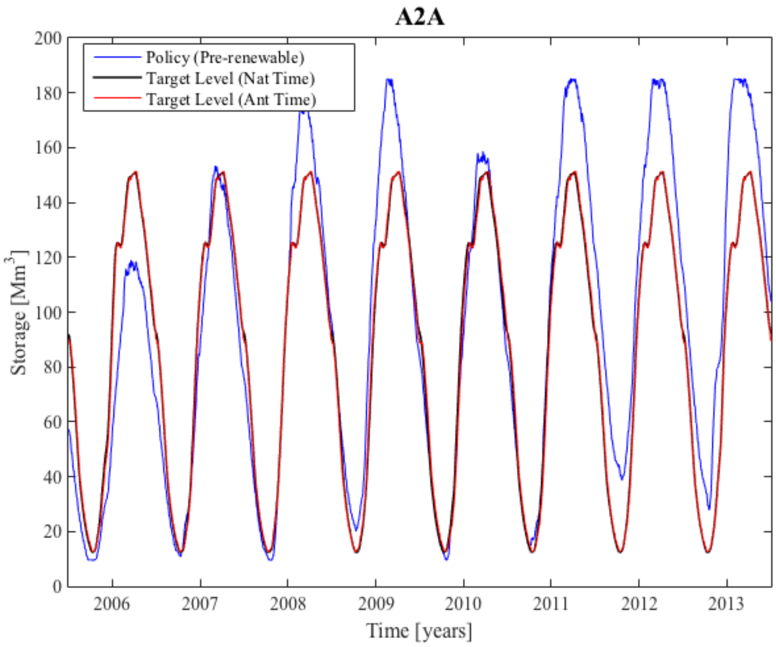

Figure 7-4: Storage obtained from different simulation modes (policy, target level based on natural time, target level based on the anthropic time) for the A2A reservoir

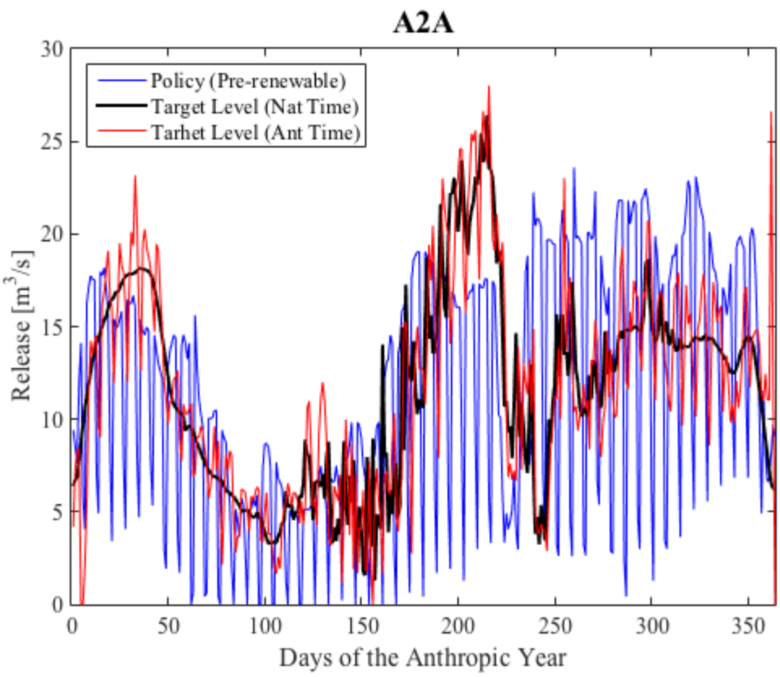

Figure 7-5: Average release per day of the anthropic year obtained by different simulation modes (policy, target level based on natural time, target level based on the anthropic time) for the A2A reservoir

7.2 Hydropower performance

Another way to assess the differences between simple and advanced reservoirs operating rules is to calculate the hydropower performance. The energy production and the revenue obtained from the selling of the energy

produced by the equivalent turbine downstream of the reservoir are determined calculating the objective function implemented in the behavioural model (see chapter 5) using the release simulated with the different simulation modes and the real prices observed in the simulation horizon (2006-2013). The results in terms of production and revenue are then normalized on the historical performances[3].
Figure 7-6 shows that the performance of the simulation based on a target level computed on the natural time and the performance of the simulation based on a target level computed on the anthropic time are almost the same: they underestimate the production of about 7% and the revenue of about 5%. The simulation based on an optimal policy, which underestimate the production of about 9%, is instead able to obtain revenue very close to the historical one.

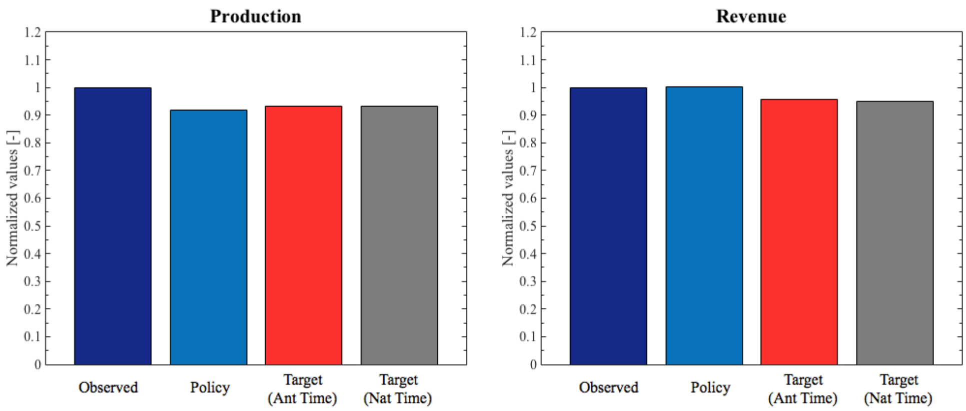

Figure 7-6: Production and revenue normalized on the observed values for different simulation modes for the A2A reservoir

7.3 Hydrological response

To assess how far from the reservoirs the release affect the hydrological regime, we check the river flow simulated in different control sections of the catchment (Figure 7-7). We compare the simulation performed using a target level based on the natural time with the simulations performed using the pre-renewable and the post-renewable optimized policies. The comparison between the pre-renewable and the post-renewable optimized policies simulations allows assessing the hydrological effects of different reservoirs management in response to changes in the socio-economic drivers (see chapter 5.3).

These effects could also be assessed simulating the reservoirs' dynamics with different target levels: one based on the pre-renewable historical observations and the other based on post-renewable historical observations. This is possible because, in our case, the changes in the socio-economic

[3] The historical performances are determined calculating the objective function implemented in the model using the historical release.

drivers already occurred in the past and the observations of the system in response to these changes are therefore available. If we wanted instead to simulate the system under future scenarios of climate or socio-economic changes, the use of target rule would bring unpredictable results and the use of an optimized policy would be necessary.

Sections A and B are located immediately downstream of the reservoirs and the flow has the same pattern of the release from the reservoirs (not shown). The other sections are instead located along the main river of the catchment, the Adda River, and the average flow per day of the anthropic year is shown in Figure 7-8.

We can notice that the flow increases from section C to section F, according to the river flow direction.
The high variability of the streamflow between weekdays and weekends, caused by the reservoirs operators, which release smaller volume of water during the weekends, when the price of the energy is lower and releasing is therefore less convenient, is well visible in the simulations based on an optimized policy. Furthermore these fluctuations are more evident in the winter months as the natural streamflow is lower. It's also interesting to notice that this behaviour affect the hydrological regime in all the sections considered, independently from the distance from the reservoirs. This means that the effects of the anthropic component are not local but are distributed throughout the basin.
The different behaviour of the reservoirs in response to changes in the energy prices is evident in all the sections, in particular in the sections C and D, where the streamflow is lower.

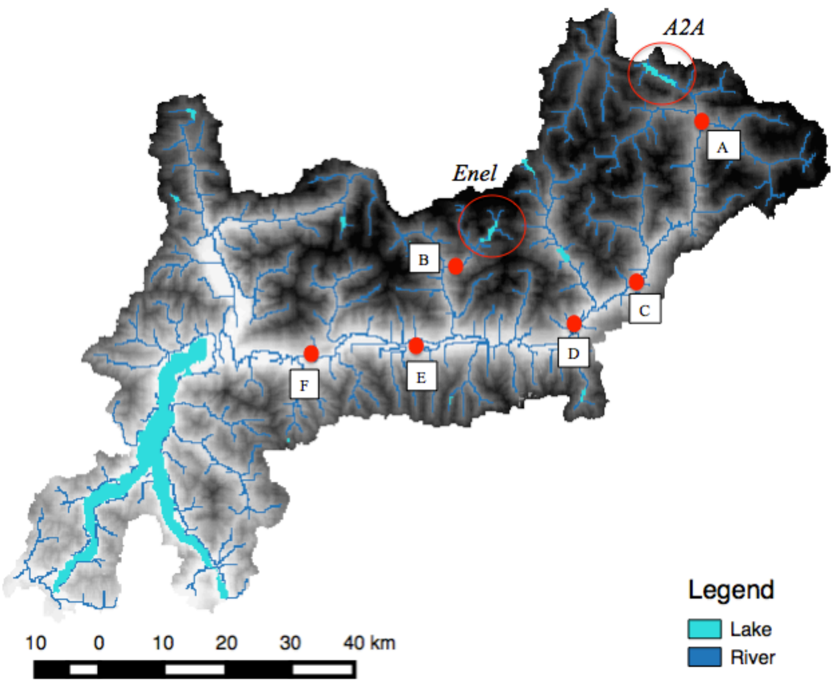

Figure 7-7: Control sections where the hydrological response is assessed

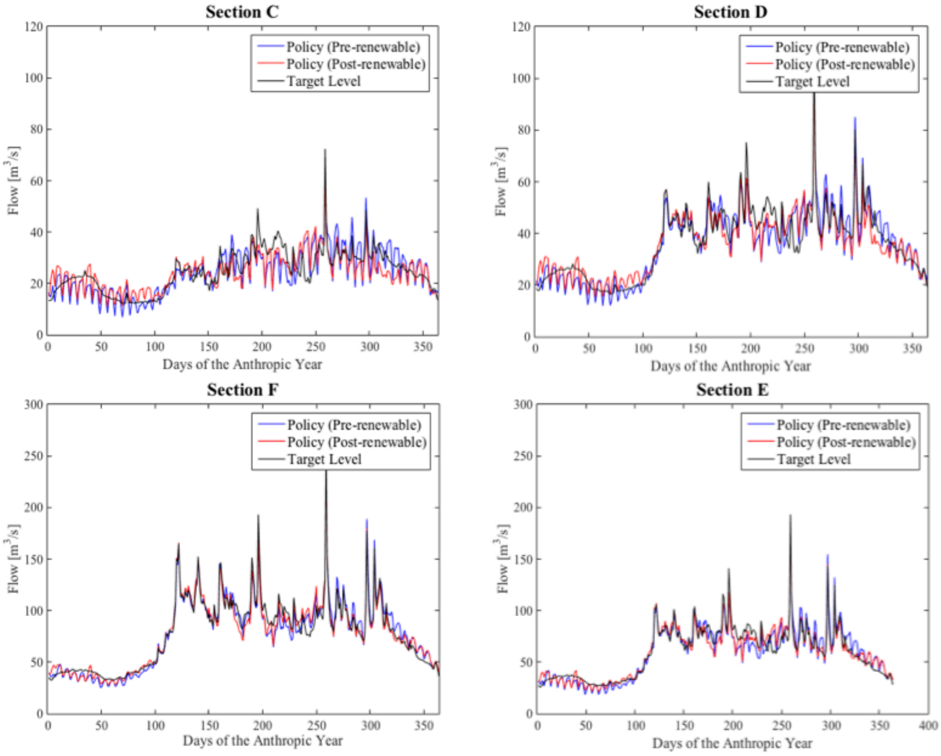

Figure 7-8: Average flow per day of the anthropic year in the control sections

8 Conclusions

The main objective of this thesis is to compare the differences that may arise from the inclusion of simple or advanced reservoirs operating rules in CHNS models in order to assess the hydropower performance and the hydrological response of the system.
More precisely we focus on an alpine basin, in which the anthropic component plays an important role and the natural hydrological cycle is deeply influenced by the presence of several hydroelectric reservoirs.

The first step of the analysis involves the calibration and validation of the hydrological model Topkapi-ETH on the inflow of the two main reservoirs of the system over the period 2003-2013: for both the reservoirs the results in validation are very satisfactory, showing values of R^2 over 0.8. The performance of the model at the only section where we have flow measurements are instead less satisfactory due to difficulties of the model in estimating the winter snowpack in some parts of the basin and in reproducing the reservoirs behaviour.

The next step consists in the modelling of hydropower operators' behaviour, generating optimized policies via SDP. These policies are strongly dependent on the energy price and are therefore able to correctly reproduce the price-dependent operators dynamics (e.g., weekdays-weekends different release). Nevertheless the model results don't always follow the historical data because we don't always know all the real operators' objectives (we consider only the revenue) and because the hydropower operators are sometimes forced to act in contrast to their interests due to non-predictable constraints imposed from outside.

The analysis of different price scenarios shows that, when the variability of the price between different periods of the year is high (e.g., pre-renewable period), the behaviour of the reservoir follows the pattern of the price, because it defines univocally when to release is more convenient. On the contrary, when the variability is low (e.g. post-renewable period), the inflow distribution, together with the price, drives the reservoir dynamics.

In order to assess the hydrological response of the system, we integrated simple reservoirs operating rules, based on the definition of a rule-curve (e.g. target level), and advancing operational policies, generated via SDP, within the hydrological model.

The analysis show that simple operating rules are usually able to reproduce the main dynamic of the reservoirs, which shift high volumes of water in space an time, but cannot capture more complex decision making processes, concerning, for example, the variability of the energy price. When the focus is not only on the hydrology but also on the hydropower is therefore preferable to simulate the reservoirs with optimized policies, which are generated solving an optimal control problem that can account for several relevant information that are usually considered in taking the decisions and therefore can better describe some decisional processes.

Moreover simple operating rules based on a rule-curve (e.g. target level) have a structural delay in capturing changes in the natural or socio economic drivers. They can just react to these changes because the observation of the behaviour of the system under the new “boundary conditions” is needed.
Reservoirs operating rules based on a rule-curve are easy to implement and they are therefore usually used in the state-of-art physically based models. When dealing with future changes in natural (e.g. climate change scenarios) or socio-economical (e.g. energy price, energy demand) drivers, these rules are no more suitable, because to anticipate the changes, modelling the relationship between the drivers and the reservoirs operators behaviour, become essential to accurately describe the system.

Future works could aim at improving both the hydrological and behavioural models.
Regarding the hydrological model, we could define the hydrometeorological inputs with more accuracy in order to better describe the processes concerning the accumulation and melting of snow and ice, which constitute one of the main issue in reproducing the observed flow.
Concerning the behavioural model, we could implement a multi-objective problem: the revenue is not in fact the only objective of the hydropower operators, who also considers, in decision processes, other aspects (e.g., energy production, balancing services).

Furthermore, analysis of climate change could permit assessing the flexibility of simple and complex reservoirs operating rules in capturing impacts on the system due to changes in the natural drivers. Since the climate change strongly affects the inflow to the reservoirs, we expect that the optimized policies, which are generated taking explicitly into account the inflow distribution, should obtain better results in describing the response of the operators behaviour to changes in the natural drivers.

Finally, we could enhance the CHNS model integrating within the hydrological model an external module able to generate on-line optimal reservoirs policies using different optimization algorithm like, for example, algorithms based on radial basis functions or artificial neural networks.

Bibliography

[Anghileri et al., 2011] Anghileri, D., Pianosi, F., and Soncini-Sessa, R. (2011). A framework for the quantitative assessment of climate change impacts on water-related activities at the basin scale. Hydrology and Earth System Science, 15.

[Anghileri et al., 2013] Anghileri, D., Castelletti, A., M.ASCE, Pianosi, F., Soncini-Sessa, R. and Weber, E. (2013). Optimizing Watershed Management by Coordinated Operation of Storing Facilities. Journal of Water Resources Planning and Management.

[Baron, 1998] Baron, J. (1998). Judgment misguided: Intuition and error in public decision making. Oxford University Press.

[Barthel et al., 2008] Barthel, R. et al. (2008). An integrated modelling framework for simulating regional scale actor responses to global change in the water domain. Environmental Modelling & Software 23.9, 1095–1121.

[Becu et al., 2003] Becu, N. et al. (2003). Agent based simulation of a small catchment water management in northern Thailand. Ecological Modelling 170.2-3, 319–331.

[Beven, 2012] Beven, K. (2012). Rainfall-Runoff Modelling, The Primer (2nd edition). Lancaster, UK: Wiley-Blackwell.

[Brock et al., 2000] Brock, B., Willis, I., and Sharp, M. (2000). Measurement and parametrization of albedo variations at Haut Glacier d'Arolla, Switzerland. Journal of Glaciology, 46(155), 675-688.

[Carenzo et al., 2009] Carenzo, M., Pellicciotti, F., Rimkus, S., and Burlando, P. (2009). Assessing the transferability and robustness of an enhanced temperature-index glacier melt model. Journal of Glaciology, 55.

[Castelletti et al., 2008] Castelletti, A., Pianosi, F. and Soncini-Sessa, R. (2008). Water reservoir control under economic, social and environmental constraints. Automatica.

[Ciarapica and Todini, 2002] Ciarapica, L. and Todini, E. (2002). Topkapi: a model for the representation of the rainfall-runoff process at different scales. Hydrolog. Proc., 16.

[Crawford and Linsley, 1966] Crawford, N. H., and R. K. Linsley (1966). Digital simulation in hydrology: Stanford watershed model IV. Tech. Rep. 39, 210. Dep. of Civ. Eng., Stanford Univ., Stanford, Calif.

[Dooge, 1955] Dooge, J. C. I. (1955). Linear Theory of Hydrological Systems. U.S. Dep. Agric. Tech. Bull. 1468, 327.

[Falkenmark, 1997] Falkenmark, M. (1997). Society's interaction with the water cycle: a conceptual framework for a more holistic approach. Hydrological Sciences Journal 42.February, 451–466.

[Farinotti et al., 2009] Farinotti, D., Huss, M., Bauder, A., and Funk, M. (2009). An estimate of the glacier ice volume in the swiss alps. Global and Planetary Change, 68.

[Fatichi et al., 2013] Fatichi, S., Rimkus, S., Burlando, P., Bordoy, R., and Molnar, P. (2013). Elevational dependence of climate change impacts on water resources in an alpine catchment. Hydrology and Earth System Science, 10.

[Fischer et al., 2014] Fischer et al. (2014). The new Swiss Glacier Inventory SGI2010. Arctic, Antarctic and Alpine Research, 46(4), 933-945.

[Giuliani and Castelletti, 2013] Giuliani, M. and Castelletti, A. (2013). Assessing the value of cooperation and information exchange in large water resources systems by agent-based optimization. Water Resources Research 49.7. 3912–3926.

[Giuliani et al., 2016] M. Giuliani, D. Anghileri, P. N. Vu, A. Castelletti, and R. Soncini-Sessa. Large storage operations under climate change: expanding uncertainties and evolving tradeoffs. Environmental Research Letters, vol. 11.

[Gupta et al., 2009] Gupta, H., Kling, H., Yilmaz, K., and Martinez, G. (2009). Decomposition of the mean squared error and nse performance criteria: Implications for improving hydrological modelling. Journal of Hydrology, 377.

[Huss and Farinotti, 2012] Huss and Farinotti (2012). Distributed ice thickness and volume of all glaciers around the globe. Journal of Geophysical Research, 117.

[Isotta et al., 2014] Isotta, F., Frei, C., and Weilguni, V. (2014). The climate of daily precipitation in the alps: development and analysis of a high-resolution grid dataset from pan-alpine rain-gauge data. International Journal of Climatology, 34.

[Kumar et al., 2009] Kumar, M., C. J. Duffy, and K. M. Salvage (2009). A second-order accurate, finite volume–based, integrated hydrologic modeling (FIHM) framework for simulation of surface and subsurface flow. Vadose Zone J., 8(4), 873–890.

[Legates and McCabe, 1999] Legates, D. and McCabe, G. (1999). Evaluating the use of goodness of fit measures in hydrologic and hydroclimatic model validation. Water resources research, 35.

[Liu and Todini, 2002] Liu, Z. and Todini, E. (2002). Towards a comprehensive physically-based rainfall-runoff model. Hydrology and Earth System Sciences, 6.

[Liu and Todini, 2006] Liu, Z. and Todini, E. (2006). Assessing the topkapi non-linear reservoir cascade approximation by means of a characteristic lines solution. Hydrological Processes, 19.

[Liu et al., 2005] Liu, Z., Martina, M. L. V., and Todini, E. (2005). Flood forecasting using a fully distributed model: application of the topkapi model to the upper xixian catchment. Hydrology and Earth System Science, 9.

[Milly et al., 2007] Milly, P. et al. (2007). Stationarity is dead. Ground Water News & Views 4.1, 6–8.

[Nickerson, 1998] Nickerson, R. S. (1998). Confirmation bias: A ubiquitous phenomenon in many guises. Review of general psychology 2.2, 175.

[Ng et al. 2011] Ng, T. L. et al. (2011). An agent-based model of farmer decision-making and water quality impacts at the watershed scale under markets for carbon allowances and a second generation biofuel crop. Water Resources Research 47.9.

[Pellicciotti et al., 2005] Pellicciotti, F., Brock, B., Strasser, U., Burlando, P., and Funk, M. (2005). An enhanced temperature-index glacier melt model including the shortwave radiation balance: development and testing for haut glacier d'arolla, switzerland. Journal of Glaciology, 51.

[Polhill et al., 2016] Polhill, J. G. et al. (2016). Modelling systemic change in coupled socio environmental systems. Environmental Modelling & Software 75, 318–332.

[Priestley and Taylor, 1972] Priestley, C. and Taylor, R. (1972). On the assessment of surface heat flux and evaporation using large-scale parameters. Monthly Weather Review.

[Sivapalan and Bloschl, 2015] Sivapalan, M., and G. Bloschl (2015). Time scale interactions and the coevolution of humans and water. Water Resour. Res., 51, 6988–7022.

[Soncini-Sessa et al., 2007] Soncini-Sessa, R., Castelletti, A., and Weber, E. (2007). Integrated and Partecipatory Water Resources Management: Theory, volume 1A.

[Therrien et al., 2010] Therrien, R., R. G. McLaren, E. A. Sudicky, and S. M. Panday (2010). HydroGeoSphere: A Three-Dimensional Numerical Model Describing Fully-Integrated Subsurface and Surface Flow and Solute Transport. Groundwater Simul. Group, Univ. of Waterloo, Waterloo, Ontario, Canada.

[Voisin et al., 2011] Voisin, N., Li, H., Ward, D., Huang, M., Wigmosta, M., and Leung, L. R. (2013). On an improved sub-regional water resources management representation for integration into earth system models. Hydrology and Earth System Science, 17.

[Wagener, 2010] Wagener, T. et al. (2010). The future of hydrology: An evolving science for a changing world. Water Resources Research 46.5, W05301.

[Wood et al., 2011] Wood, E. F., et al. (2011). Hyper-resolution global land surface modeling: Meeting a grand challenge for monitoring Earth's terrestrial water. Water Resour. Res., 47.

[Yevjevich, 1972] Yevjevich, V. (1972). Stochastic Processes in Hydrology, 276. Water Resour. Publ., Littleton, Colo.

Bibliography